Gmail **Maiten Lafuente Diaz <maitenlafuentediaz@gmail.com>**

IJPS Ms. 44709R1

1 mensaje

Carla J. Harper <em@editorialmanager.com> 16 de diciembre de 2020 a las 12:15
Responder a: "Carla J. Harper" <charper@tcd.ie>
Para: "Maiten A. Lafuente Diaz" <maitenlafuentediaz@gmail.com>

Dear Dr. Lafuente Diaz:

I am pleased to inform you that your manuscript entitled "FTIR spectroscopy studies in Cretaceous gymnosperms from the Santa Cruz province, Patagonia, Argentina" has been accepted for publication in the *International Journal of Plant Sciences*. I also want to thank the authors for their prompt revisions and improvements to the manuscript.

Thank you all once again for your contribution to the special volume.

The Journal Office will now double-check the quality of the image files and also ensure that a completed Publication Agreement has been received. Once this is done, the files will be sent to the publisher for editing and typesetting, and the proofs will be made available for your review (about 8 weeks prior to print publication).

In the interim, your manuscript will soon be posted online as a "preprint" on our Just Accepted page. Shortly after the proofs have been served, returned and corrected, your article will be available electronically on the journal's Ahead of Print page.

Thank you for publishing in the *International Journal of Plant Sciences*.

Sincerely,

Carla J. Harper, Ph.D.
Guest Editor
INTERNATIONAL JOURNAL OF PLANT SCIENCES

OPEN ACCESS: *IJPS* authors have the option to make their accepted paper freely available online immediately upon publication. The fee for Gold Open Access (published under CC-BY-NC-4.0 license) is $1,300; discounted to $400 if the lead author's institution subscribes to the journal. Requests for Open Access must be made soon (no later than 45 days from today). Write to ijps@uchicago.edu for instructions.

FREE SUBSCRIPTION: If you and another author of this paper wish to receive a complimentary 12-month subscription to the electronic edition of *IJPS*, please send two e-mail and postal addresses (no P.O. boxes) to ijps@uchicago.edu.

NOMENCLATURE: Articles that introduce new taxonomic names should not be posted online prior to proof correction. In addition, no changes to the article can be made after publication online Ahead of Print. If you wish to skip the early "preprint" publication of your article, please alert the journal staff at ijps@uchicago.edu immediately so that we can omit that process.

International Journal of Plant Sciences

FTIR spectroscopy studies in Cretaceous gymnosperms from the Santa Cruz province, Patagonia, Argentina

--Manuscript Draft--

Article Type:	Special Issue - Women in Paleobotany
Manuscript Number:	44709R1
Full Title:	FTIR spectroscopy studies in Cretaceous gymnosperms from the Santa Cruz province, Patagonia, Argentina
Corresponding Author:	Maiten A. Lafuente Diaz Museo Argentino de Ciencias Naturales Bernardino Rivadavia Ciudad Autónoma de Buenos Aires, Ciudad Autónoma de Buenos Aires ARGENTINA
Corresponding Author's Institution:	Museo Argentino de Ciencias Naturales Bernardino Rivadavia
Other Authors:	Georgina M. Del Fueyo, Dr.
	José A. D'Angelo, Dr.
	Martín A. Carrizo, Dr.
Abstract:	Premise of the Research. In this contribution, the spectroscopic characterization of Gymnosperms fossil remains belonging to Pteridospermophyta, Cycadophyta, Ginkgophyta, and Coniferophyta collected from the Anfiteatro de Ticó and Punta del Barco formations (Baqueró Group; Aptian) and Springhill (Hauterivian-Barremian) and Piedra Clavada/Kachaike (Albian) formations, outcropping in the Santa Cruz province, Argentina is presented. From these lithostratigraphic units, specimens of several fossil taxa showing the existence of a diverse plant assemblage during the Lower Cretaceous in Patagonia were selected. Methodology. The fossils consist of foliar compressions with very well-preserved cuticles that are chemically characterized by Fourier Transform Infrared (FTIR) spectroscopy. Foliar remains are analyzed into two sample forms: 1) compressions (including coalified mesophyll and cuticle; Cp) and 2) cuticles (Ct). Additionally, semiquantitative data are evaluated through Principal Component Analysis (PCA) revealing the functional groups preserved at the mesophyll and cuticle levels for each analyzed fossil taxa. Pivotal Results. In general, the species from the Baqueró Group show similar chemical compositions between the Cp and Ct sample forms whereas the chemistry of the foliar compressions from the Springhill and Piedra Clavada/Kachaike formations reveals the presence of a high contribution of aromatic structures making up the cuticles. Conclusions. The compressions of Pseudoctenis ornata , Ginkgoites tigrensis , and Squamastrobus tigrensis probably underwent, during and after diagenesis, a natural oxidation process most likely caused by the recurrent volcanic activity occurred during the Aptian sedimentation of the Baqueró Group. In contrast, Ruflorinia orlandoi , Ptilophyllum micropapillosum , and Ginkgoites skottsbergii have cuticles presumably composed of highly aromatic structures (such as phenylpropanoids and aromatic domains) in cutins and cutans as well due to the presence of other phenolic compounds. A new term is here proposed for Ginkgoites skottsbergii : vitrinitic compression, while P seudoctenis ornata , Ginkgoites tigrensis, Squamastrobus tigrensis, Ptilophyllum micropapillosum , and Ruflorinia orlandoi are called liptinitic compressions.
Author Comments:	The cover letter mentioned a version including all the changes made with the Track Changes option. This file is submitted as Response to reviwers.
Additional Information:	
Question	**Response**

Buenos Aires, December 10 2020

Dr. Carla J. Harper
Guest Editor
International Journal of Plant Sciences

Dear Dr. Harper,

I send you the revised version of the manuscript **IJPS Ms. 44709** "FTIR spectroscopy studies in Cretaceous gymnosperms from the Santa Cruz province, Patagonia, Argentina" by Maiten A. Lafuente Diaz, Georgina M. Del Fueyo, José A. D'Angelo, and Martín A. Carrizo to be considered for publication in the Special Issue celebrating Women in Paleobotany: A Tribute to Edith L. Taylor of the International Journal of Plant Sciences dedicated to Prof. Edith L. Taylor.

I have made all of the corrections suggested by you that have undoubtedly improved the manuscript. In this case, no responses to comments and suggestions are included.

Finally, I send you the final version and the marked version of the manuscript. The latter version includes all the changes made with the Track Changes option.

I hope you find this new version of the article suitable for publication in the Special Issue of the International Journal of Plant Sciences.

Thank you in advance for your attention.

Sincerely yours

Maiten A. Lafuente Diaz
División Paleobotánica
Museo Argentino de Ciencias Naturales
"Bernardino Rivadavia" – CONICET
Av. Ángel Gallardo 470
C1405DJR, Buenos Aires, Argentina
e-mail: maitenlafuentediaz@gmail.com

FTIR spectroscopy studies in Cretaceous gymnosperms from the Santa Cruz province, Patagonia, Argentina

Maiten A. Lafuente Diaz[1,*], Georgina M. Del Fueyo[1], José A. D'Angelo[2,3], Martín A. Carrizo[1]

[1]Museo Argentino de Ciencias Naturales "Bernardino Rivadavia"-CONICET, Avda. Ángel Gallardo 470, C1405DJR, Ciudad Autónoma de Buenos Aires, Argentina. maitenlafuentediaz@gmail.com, georgidf@yahoo.com.ar, blackdisc@gmail.com

[2]IANIGLA-CCT-CONICET-MENDOZA. Área de Química, FCEN, Universidad Nacional de Cuyo, M5502JMA, Mendoza, Argentina.

[3]Palaeobotanical Laboratory, Cape Breton University, 1250 Grand Lake Rd., Sydney, Nova Scotia B1P 6L2, Canada. joseadangelo@yahoo.com,

*Corresponding author:

Family name: Lafuente Diaz

First and second names: Maiten Amalia

Postal address: Av. Ángel Gallardo 470, (C1405DJR) Buenos Aires, Argentina.

Telephone number: + 54- 011-4982-6595

E-mail address: maitenlafuentediaz@gmail.com

Running head: Lafuente Diaz et al.- FTIR studies of Cretaceous plants

Premise of the Research. In this contribution, the spectroscopic characterization of Gymnosperms fossil remains belonging to Pteridospermophyta, Cycadophyta, Ginkgophyta, and Coniferophyta collected from the Anfiteatro de Ticó and Punta del Barco formations (Baqueró Group; Aptian) and Springhill (Hauterivian-Barremian) and Piedra Clavada/Kachaike (Albian) formations, outcropping in the Santa Cruz province, Argentina is presented. From these lithostratigraphic units, specimens of several fossil taxa showing the existence of a diverse plant assemblage during the Lower Cretaceous in Patagonia were selected.

Methodology. The fossils consist of foliar compressions with very well-preserved cuticles that are chemically characterized by Fourier Transform Infrared (FTIR) spectroscopy. Foliar remains are analyzed into two sample forms: 1) compressions (including coalified mesophyll and cuticle; Cp) and 2) cuticles (Ct). Additionally, semiquantitative data are evaluated through Principal Component Analysis (PCA) revealing the functional groups preserved at the mesophyll and cuticle levels for each analyzed fossil taxa.

Pivotal Results. In general, the species from the Baqueró Group show similar chemical compositions between the Cp and Ct sample forms whereas the chemistry of the foliar compressions from the Springhill and Piedra Clavada/Kachaike formations reveals the presence of a high contribution of aromatic structures making up the cuticles.

Conclusions. The compressions of *Pseudoctenis ornata*, *Ginkgoites tigrensis*, and *Squamastrobus tigrensis* probably underwent, during and after diagenesis, a natural oxidation process most likely caused by the recurrent volcanic activity occurred during the Aptian sedimentation of the Baqueró Group. In contrast, *Ruflorinia orlandoi*, *Ptilophyllum micropapillosum*, and *Ginkgoites skottsbergii* have cuticles presumably composed of highly aromatic structures (such as phenylpropanoids and aromatic domains) in cutins and cutans as well due to the presence of other phenolic compounds. A new term is here proposed for *Ginkgoites skottsbergii*: vitrinitic compression, while *Pseudoctenis ornata*, *Ginkgoites*

tigrensis, Squamastrobus tigrensis, Ptilophyllum micropapillosum, and *Ruflorinia orlandoi* are called liptinitic compressions.

Keywords: Compression, Cuticle, FTIR spectroscopy, Gymnosperms, Lower Cretaceous, Patagonia.

INTRODUCTION

Plant fossil remains are usually morphologically, anatomically, and ultrastructurally studied. In addition, these materials constitute a suitable source from which it is possible to obtain unknown chemical information of plants that inhabited in the past. Among several chemical analytical techniques, Fourier transform infrared (FTIR) spectroscopy is particularly relevant. Over the last decades, the quantity of papers using FTIR spectroscopy in order to analyze the preserved chemistry in coalified plant fossil remains, also known as compressions, has increased significantly.

Spectroscopic analyzes have been applied from different approaches. Among them, the preservation types and paleochemotaxonomy of plant fossil remains as well as paleoenvironmental, diagenetic, and postdiagenetic conditions involved in fossilization processes have been mainly analyzed (e.g., Zodrow and Mastalerz, 2009; D'Angelo and Zodrow, 2015; Zodrow et al., 2016; Lafuente Diaz et al., 2018a, 2019a, 2020a; Zodrow and Mastalerz, 2019, among others). These investigations have been predominantly carried out on Pennsylvanian gymnosperms, vegetative and reproductive organs from the Sydney Coalfield, Canada and, to a lesser extent, on plant remains from the Devonian, Carboniferous, and Triassic of Canada, the Czech Republic, Spain, and Brazil, among others (e.g., Pšenicka et al., 2005; Zodrow et al., 2009; D'Angelo and Zodrow, 2015; Matsumura et al., 2016). Among the latest analyzes, a chemical representation of the fertile structures of *Trigonocarpus grandis* in organic connection to vegetative organs has been obtained (Zodrow et al., 2013). Also, the possible relation between the architecture of the fronds and the functional groups in the genera *Alethopteris* and *Neuropteris* has been revealed by Zodrow et al. (2017) and D'Angelo and Zodrow (2018a), whereas the phytochemistry of the biomacropolymers of the *Macroneuropteis macrophylla* cuticle has been determined by Zodrow et al. (2010) and D'Angelo et al. (2013). Recently, Zodrow and Mastalerz (2019) have established a new preservation type for the pollen organ of *Dolerotheca* (Medullosales).

On the other hand, the compressions of plant fossils from Argentina have also been studied using FTIR spectroscopy, such as the cases of the *Dicroidium* flora from the Triassic of the Mendoza province (e.g., D'Angelo et al., 2011; D'Angelo and Zodrow, 2018b; D'Angelo, 2019). Among others, the chemical structure of the *Johnstonia coriacea* cutin has been determined (D'Angelo and Zodrow, 2018b), whereas the study of *Dicroidium* flora has evaluated the possibility of ecophysiological adaptations in the *Dicroidium* and *Johnstonia* genera (D'Angelo, 2019). However, in recent times, a comprehensive analysis of plant fossil remains from the Lower Cretaceous of Patagonia has begun to be performed through the use of FTIR spectroscopy in conjunction with morphological and anatomical studies (Lafuente Diaz, 2019).

In this contribution, the spectroscopic characterization of gymnosperm fossil remains collected from three Cretaceous lithostratigraphic units outcropping in the Santa Cruz province is analyzed and compared. These units are the Anfiteatro de Ticó and Punta del Barco formations of the Baqueró Group and the Springhill and Piedra Clavada/Kachaike formations. From them, six fossil taxa belonging to different plant groups were selected in order to compare the chemical compositions of the fossil taxa and to reveal the similarities or differences among them. In turn, the chemical compositions are interpreted in relation to the probable original chemistry of the plants and the prevailing paleoenvironmental conditions during the deposition of the different formations.

The gymnosperm fossil taxa chemically analyzed herein will contribute to increase the knowledge about the spectroscopic studies applied to plant fossils from Patagonia, as well as achieve a comprehensive understanding of the plant communities that inhabited that area during the Lower Cretaceous.

MATERIALS AND METHODS

Materials and provenance

The materials comprise foliar compressions of six fossil taxa that were collected in three Cretaceous lithostratigraphic units outcropping in the Santa Cruz province, Argentina

(Fig. 1). The specimens are the conifer *Squamastrobus tigrensis* Archangelsky and Del Fueyo (Coniferophyta), the cycadal *Pseudoctenis ornata* Archangelsky et al. (Cycadophyta) and the ginkgoal *Ginkgoites tigrensis* Archangelsky (Ginkgophyta) from the Baqueró Group, the bennettital *Pilophyllum micropapillosum* Lafuente Diaz, Carrizo and Del Fueyo (Cycadophyta), and the pteridosperma *Ruflorinia orlandoi* Carrizo and Del Fueyo (Pteridospermophyta) from the Springhill Formation, and the ginkgoal *Ginkgoites skottsbergii* Lundblad (Ginkgophyta) from the Piedra Clavada/Kachaike Formation.

The provenance of the fossil species and the particular paleoenvironments where the parent plants grown during the Lower Cretaceous of Patagonia are listed below.

Baqueró Group. The Baqueró Group (Cladera et al., 2002) is a predominantly volcanic sequence that outcrops in the central region of the Santa Cruz province, Patagonia, Argentina. This Aptian lithostratigraphic unit is world-renowned for having abundant plant remains that mainly include compressions with exceptionally well-preserved cuticles (Archangelsky, 2003; Del Fueyo et al., 2007; Llorens et al., 2020). In general, the formations that make up this group reflect river and lake systems, strongly influenced by the volcanic activity, whose deposits consist of sandstones, conglomerates, tuffs, and mudstones (Cladera et al., 2002; Limarino et al., 2012).

Among the fossil taxa studied spectroscopically, *Ginkgoites tigrensis* Archangelsky and *Squamastrobus tigrensis* Archangelsky and Del Fueyo were collected in the Anfiteatro de Ticó Formation (basal unit) at the Bajo Tigre fossiliferous locality. The conifer *S. tigrensis* was recovered from the Bajo Tigre *Otozamites* (BTO) fossiliferous level, which consists of siliciclastic and volcaniclastic lithofacies, while the materials of *G. tigrensis* were collected from the Bajo Tigre *Ginkgoites* (BTG) fossiliferous level, which is composed by volcanic tuffs (Archangelsky, 1965; Archangelsky and Del Fueyo, 1989). The Anfiteatro de Ticó Formation was dated by Perez Loinaze et al. (2013), estimating a late Aptian age of 118.23 ± 0.09 Ma. On the other hand, *Pseudoctenis ornata* was recuperated from the Punta del Barco Formation (upper unit) at the Estancia El Verano fossiliferous locality in the homonymous fossiliferous level that comprises volcanic tuffs (Archangelsky et al., 1995).

The age of this lithostratigraphic unit was constrained to the late Aptian in accordance with the dating age of 114.67 ± 0.18 Ma (Césari et al., 2011).

Springhill Formation. The deposits of the Springhill Formation (Thomas, 1949) outcrop saltatory in restricted areas of the Santa Cruz province, among which the Río Correntoso locality near the Lake Ghío comprise several fossiliferous levels singularly rich in fossils. The strata in this locality, of continental origin, are interpreted as fluvial deposits which consist of coarse-to-fine grained quartz sandstones with variable intercalations of shale (Carrizo et al., 2014). In particular, the plant fossil remains belonging to *Ruflorinia orlandoi* Carrizo and Del Fueyo and *Ptillophyllum micropapillosum* Lafuente Diaz, Carrizo, and Del Fueyo were collected from a pelitic fossiliferous level at the Río Correntoso locality.

The Springhill Formation deposits exhibit marked heterochrony from the late Jurassic to Barremian due to their extensive areal distribution (e.g., Riccardi, 1971; Archangelsky et al., 1981; Riccardi, 1988; Riccardi et al., 1992; Ottone and Aguirre-Urreta, 2000). The age of the Springhill Formation at the Estancia El Salitral fossiliferous locality was established as Hauterivian-Barremian (Archangelsky et al., 1981; Carrizo and Del Fueyo, 2015; Ottone and Aguirre-Urreta, 2000). Because the outcrops of this unit in the Río Correntoso fossiliferous locality are in the vicinity of the Estancia El Salitral locality they are also considered of the Hauterivian-Barremian age (Carrizo et al., 2019).

Piedra Clavada/Kachaike Formation. In the Lake San Martín area, the Piedra Clavada/Kachaike Formation outcrops east of the homonymous lake from the Río de los Fósiles in the north to Estancia Kachaike in the south. The age of this lithostratigraphic unit is based on several palynological studies (Barreda and Archangelsky, 2006; Villar de Seoane and Archangelsky, 2008; Archangelsky et al., 2012) and the presence of ammonites and microplankton (Aguirre-Urreta, 2002; Guler and Archangelsky, 2006) that constraint the Piedra Clavada/Kachaike Formation to the Albian.

Ginkgoites skottsbergii Lundblad was collected at the Bajo Comisión fossiliferous locality, Estancia Sierra Nevada (Santa Cruz province, Argentina). The fossiliferous level corresponds to continental deposits that are composed of sandstones

from a fluvial environment, i.e., a floodplain (Archangelsky et al., 2012; Del Fueyo et al., 2008).

Repositories. The fossil specimens from the Baqueró Group and the Piedra Clavada/Kachaike Formation, used both for FTIR spectroscopy and for morpho-anatomical studies, are housed in the Paleobotany Collection of the Museo Argentino de Ciencias Naturales ‘‘Bernardino Rivadavia’’ under the acronyms: BA Pb (Megascopic and FTIR Spectroscopy Samples) and BA Pb SEM (Scanning Electron Microscopy: SEM). The materials used for each fossil taxon are specified as follows: 1) *Pseudoctenis ornata* BA Pb 1217, 1220, 1222 and BA Pb MEB 643, 645-646; 2) *Ginkgoites tigrensis* BA Pb 11556-11557, 11561, 14880, 14883, 14887-14889, 14890 and BA Pb MEB 589; 3) *Squamastrobus tigrensis* BA Pb 7678, 11321, 11324, 11333, 11583-11586 and BA Pb MEB 585; and 4) *Ginkgoites skottsbergii* BA Pb 13850 and BA Pb MEB 249.

On the other hand, the fossil specimens collected in the Springhill Formation and used for FTIR spectroscopy and morpho-anatomical studies are deposited in the Paleobotany Collection of the Museo Regional Provincial “Museo Padre Jesús Molina” under the acronym MPM Pb (fossil specimens and samples for SEM). For *Ruflorinia orlandoi*, the samples are MPM Pb 15313, 15323-15330, and 15333, while for *Ptillophyllum micropapillosum* the material is MPM Pb 15355.

Methods

Fourier Transform Infrared (FTIR) spectroscopy

Sampling and sample forms. The sampling was differentially carried out according to the particularities of each fossil taxon as well as the material availability. (Table 1).

In general, to remove silicates and other inorganic compounds, the samples were treated with 36.5-38.0% hydrochloric acid (HCl) followed by 70% hydrofluoric acid (HF) and a final treatment with HCl at 36.5-38.0%.

The treated samples were subdivided into two portions defining two chemical sample forms: compressions (Cp) and cuticles (Ct). For this purpose, a portion was

retained without additional treatment to obtain the Cp samples that are composed of the adaxial and abaxial cuticles and the coalified mesophyll between them. The remaining portion was oxidized using 50% sodium hypochlorite (NaClO) for approximately 2 minutes to eliminate mesophyll remnants and thus forming the Ct samples. The latter consist of the adaxial and abaxial cuticles (Fig. 2).

Potassium bromide (KBr) pellets, composed of approximately 1-2 mg of fossil material in 250 mg of KBr, were used to acquire Cp and Ct spectra. From each KBr pellet, a single spectrum was obtained using in part a Burker EQUINOX 55 FTIR equipment with a DLATGS detector and a KBr beam splitter, which accumulated 64 scans (CEQUINOR-CONICET), and in part a Nicolet Thermo-Electron infrared spectrometer 6700 which accumulated 256 scans (FQByF-UNSL). Both spectrometers used a resolution of 4 cm^{-1} at a wavenumber range between 4000 cm^{-1} and 400 cm^{-1}.

FTIR spectra and statistical analysis. From the FTIR spectra, qualitative and semi-quantitative data of the functional groups present in Cp and Ct samples of the selected fossil taxa were obtained. The qualitative analysis included the assignments of functional groups regarding the wavenumbers in which the main functional groups and classes of compounds absorb (Table 2; Colthup et al., 1990; Ingle and Crouch, 1988; Wang and Griffiths, 1985). Figure 3 shows a representative spectrum of the most important functional groups that occur in plant fossils.

The semi-quantitative data were obtained from the determination of peak-area ratios employing the measurements of the total content of certain functional groups. The latter were carried out by integrating the total area under the peaks in the following regions: (1) CHal: aliphatic (3000-2800 cm^{-1}), (2) Ox: oxygen-containing compounds (1800-1600 cm^{-1}; the combined contribution of C=O and C=C bonds), (3) individual contributions of carbonyl/ carboxyl (C=O; 1700-1600 cm^{-1}) groups, and (4) aromatic carbon (C=C; 1600-1500 cm^{-1}) structures. The definitions of the semi-quantitative data (peak-area ratios), together with the band regions employed for calculation and

interpretation, are summarized in Table 3. The semi-quantitative IR information was refined and enhanced on digitized spectra using well-known techniques for processing signals (i.e., Fourier self-deconvolution procedure, area integration methods, and calculation of peak-area ratios) according to the procedures used by D'Angelo et al. (2010), Zodrow et al. (2009), among others.

The semi-quantitative data of the six fossil taxa were organized into a data matrix which was statistically analyzed using Principal Component Analysis (PCA), following the methodology detailed in D'Angelo et al. (2010) and D'Angelo and Zodrow (2016), among others. The PCA is used to evaluate the sample groupings based on functional groups (chemical structure) and the sample forms (Cp and Ct) in terms of FTIR chemical parameters. In this contribution, the PCA was performed using OriginPro 9.0. ® software and the first three principal components (CPs) were retained. This number of CPs was established following the modified Kaiser's rule that considers retaining those CPs with eigenvalues greater than 0.7 (Jolliffe, 2002; Izenman, 2008). The first three Cps explained a cumulative variance of 88.59%.

FTIR data of the gymnosperm fossil taxa in relation to coal macerals and kerogen types. Two semi-quantitative data (PCA variables), i.e., 'A' and 'C' Factors, were used to relate the chemical composition (functional groups) of the plant fossil remains with the coal macerals and the different types of associated kerogens.

For this purpose, according to the methodology used by Lafuente Diaz et al. (2020a), ‘A’ Factor vs. 'C' Factor plots were performed following Ganz and Kalkreuth (1987; see Guo and Bustin, 1998). These plots are analogous to the traditional van Krevelen diagrams (H/C vs O/C) indicating similarities between different types of kerogen and maceral groups: liptinite, vitrinite, and inertinite. Thus, 'A' and 'C' Factors were analyzed together with some FTIR coal data available in the literature. The latter comprise liptinite, vitrinite, and inertinite macerals (thermal maturity, RO max. 0.52% - 1.41%). The data of the sporinite, cutinite, vitrinite, semifusinite, and fusinite macerals were taken from Mastalerz

and Bustin (1996), while the data for cutinite, resinite, bituminite, alginate, and vitrinite from Guo and Bustin (1998).

RESULTS

Cretaceous gymnosperm taxa studied by means of FTIR spectroscopy

Brief morpho-anatomical characterization of the fossil species. The main morphological, anatomical, and ultrastructural characteristics of the studied specimens belonging to the six fossil taxa (*Ginkgoites tigrensis, G. skottsbergii, Pseudoctenis ornata, Ptilophyllum micropapillosum, Ruflorinia orlandoi, Squamastrobus tigrensis*) are detailed in Table 4 and illustrated in Figure 4.

FTIR spectroscopy chemical characterization

Qualitative data from FTIR spectra. The representative FTIR spectra of the six taxa considering the two sample forms (Cp and Ct) are shown as supplementary data in Figures A1, A2, and A3 (Appendix A). Regardless of the sample forms, the spectra exhibited common functional groups which are detailed below.

In general, the six fossil taxa present a broad and intense band attributable to the hydroxyl group (-OH) stretch in alcohols and phenols. This peak is centered between 3445-3380 cm^{-1}. In the 3000-2600 cm^{-1} region, two peaks occur corresponding to methylene (CH_2) stretching: antisymmetric (2930-2920 cm^{-1}) and symmetric (2855-2850 cm^{-1}). At the oxygen-containing compounds zone, the cuticles and compressions of all fossil taxa show peaks assigned to C=O stretch (carbonyl/carboxyl groups; 1730-1700 cm^{-1}) and C=C stretch in aromatic compounds (1645-1600 cm^{-1}). Most of the spectra of the Cp samples of *Pseudoctenis ornata*, *Squamastrobus tigrensis*, and *Ginkgoites skottsbergii* show an acute peak of low intensity (Baqueró Group: 1515 cm^{-1} and Piedra Clavada/Kachaike Formation: 1540 cm^{-1}), which is attributable to aromatic or unsaturated structures (e.g., benzene ring in aromatic compounds). Furthermore, bands of medium to low intensity assigned to

bending vibrations (deformations) of aliphatic C-H stretch are present in all spectra. Among them, CH_2 scissor deformations (1470-1440 cm^{-1}; absent in *G. skottsbergii*), asymmetric deformations of methyl (CH_3; 1400-1370 cm^{-1}), and peaks of asymmetric stretching of C-O-C and C-O bonds corresponding to aliphatic and/or aromatic ethers. Finally, in the aromatic zone, peaks occur at 870-745 cm^{-1} indicating C-H out-of-plane bending vibrations in aromatic compounds for the most taxa spectra, with the exception of those of *P. ornata*. Additionally, in this zone and in most fossil taxa, low intensity peaks occur representing CH_2 rocking vibrations in hydrocarbons at 730-720 cm^{-1} (except *G. tigrensis* and *G. skottsbergii*). In particular, the spectra of the taxa of the genus *Ginkgoites* have high intensity peaks that could be attributed to bending vibrations in C=C-H and/or C-OH stretch reflecting alkenes and alcohols, and also, to ring deformation of aromatic compounds (685, 682, 629, 588-585 cm^{-1}).

Principal component analysis (PCA). The semi-quantitative data set derived from FTIR spectroscopy of the six taxa (Table B1, Appendix B) was analyzed by PCA (See PCA solution in Appendix C). The first three CPs account for 88.59% cumulative variation. The PCA plots of component loadings and component scores are shown in Figures 5 (PC1 vs PC2) and 6 (PC1 vs PC3).

PC 1 (explained variance 57.87%) has positive loadings on most variables (i.e., 'C' Factor, C=O cont, 'A' Factor, C=O/C=C, CHal/C=C, CH_2/CH_3, and CHal/Ox) and negative loadings on C=C cont and CHal/C=O (Fig. 5A-B). This pattern reflects the presence of functional groups of aromatic carbon and low cross-linking of polymeric structures versus aliphatic- and oxygen-containing functionalities.

It is observed for all fossil taxa that Ct samples are more variable than those of compressions from which cuticles are derived. In particular, the *Ruflorinia orlandoi* cuticles show the highest variability with respect to the PC 1 (x-axis) of all fossil species. In this case, the highest negative values are exhibited by the rachis samples Ct5 R and Ct1 R, which, in turn, have the highest values of C=C cont (and the lowest of C=O

cont). On the other hand, two specimens, Ct6, Ct7a, and Ct7b, have cuticles with positive values for PC 1, reflecting the highest values of C= O cont (and the lowest values of C=C cont) and 'A' Factor of the *R. orlandoi* cuticles.

Most of the samples of both sample forms (Cp and Ct) of *Ptilophyllum micropapillosum* and *Ruflorinia orlandoi*, as well as all samples of the genus *Ginkgoites*, show negative values against PC 1 (Fig. 5C-D). Among the cuticle samples of the two fossil taxa from the Springhill Formation, there are those that show the most negative values of the all analyzed taxa. This fact indicates that the cuticles of *P. micropapillosum* and *R. orlandoi* have a high content of aromatic functional groups (C=C cont) and a relatively low contribution of aliphatic- and oxygen-containing compounds ('A' Factor, 'C' Factor, C=O/C=C, C=O cont, CHal/Ox, and CHal/C=C) (Table B1, Appendix B).

Among the fossil taxa from the Baqueró Group, the Cp and Ct samples of *Ginkgoites tigrensis* have negative values against PC 1 as a consequence of the high contribution of C=C bonds and high values of the CHal/C O ratio. On the other hand, for *Pseudoctenis ornata* and *Squamastrobus tigrensis*, all the Cp and Ct samples have positive values against PC 1. This fact reveals that these two fossil taxa are characterized by an aliphatic nature and the high content of oxygen-containing compounds. Furthermore, it is observed that most of the *S. tigrensis* cuticles and those of *P. ornata* have an aliphatic nature greater than their respective compressions. In contrast, the *P. ornata* and *S. tigrensis* Cp samples have a greater contribution of C=C bonds in aromatic compounds than the Ct samples.

In contrast, the Cp sample of *Ginkgoites skottsbergii* is the most aromatic foliar compression of the six fossil taxa spectroscopically studied.

PC 2 (explained variance 20.88%) shows a negative loading on 'C' Factor and positive for the remaining variables, among which the highest loadings occur on CHal/Ox, CHal/C=O, CH_2/CH_3, and C=C cont (Fig. 5A-B, y-axis). This PC shows the abundance of aliphatic groups having long, unbranched polymethylenic chains with a

variable contribution of oxygen-containing compounds and low cross-linking of polymeric structures.

The Cp samples of the fossil taxa from the Springhill and Piedra Clavada/Kachaike formations as well as the Cp samples of *Ginkgoites tigrensis* (Anfiteatro de Ticó Formation) have negative values against PC 2. These samples are characterized by relatively short and branched chains of aliphatic structures (low CH_2/CH_3 values) and a high combined contribution of oxygen-containing groups and aromatic carbon (low CHal/Ox values). The latter is due to the higher content of carboxyl/carbonyl groups (C=O cont) in Cp samples. Considering the compressions of the Baqueró Group, the *Squamastrobus tigrensis* specimens fluctuate adopting negative and positive values against PC2, indicating that the foliar compressions of this conifer are variable in the relative contribution of aliphatic compounds regarding the carbonyl/carboxyl groups and aromatic carbon structures. In contrast, the *Pseudoctenis ornata* Cp samples show positive values against PC 2; these samples are the most aliphatic foliar compressions of all analyzed fossil taxa.

On the other hand, most of the cuticles, regardless of their provenance, have positive values against PC 2 (except *Ginkgoites tigrensis* [Ct4], *Squamastobus tigrensis* [Ct7a], and *Ptilophyllum micropapillosum* [8Ct-B]). This fact reflects that cuticles have an aliphatic nature. However, a certain degree of variability in the contribution of aliphatic structures and oxygen-containing and aromatic carbon functionalities is observed among the different fossil taxa. In particular, the Ct samples of *Ruflorinia orlandoi* and *P. micropapillosum* are characterized by low cross-linking of polymeric structures (high CHal/C=O values).

PC 3 (explained variance 9.85%) has positive loadings on CH_2/CH_3, and to a lesser extent on C=O cont, 'A' Factor, 'C' Factor, and CHal/Ox, and negative loadings on CHal/C=C, C=O/C=C, CHal/C=O, and C=C cont (Fig. 6A-B, y-axis). This pattern reflects the presence of relatively longer and unbranched aliphatic chains versus functional groups with variable contributions of oxygen-containing compounds and

aromatic carbon.

In all fossil taxa, a wider variability in Ct samples is observed than in those of Cp (Fig. 6C-D, y-axis). The *Ruflorinia orlandoi* Ct samples are particularly variable. Among them, some Ct samples have high negative values against PC 3, with short and branched aliphatic structures (low values of CH_2/CH_3; e.g., Ct1 R, Ct5 R). This fact reflects a high content of C=C bonds in aromatic compounds of rachis samples. In turn, the pinnae samples Ct7a and Ct7b record high positive values against PC 3 due to having the lowest values of C=C cont of this fossil taxon.

The compressions of *Pseudoctenis ornata* and *Squamastrobus tigrensis* have positive values against PC 3 due to their high aliphatic nature. The *P. ornata* Cp samples show the highest CH_2/CH_3 values of all fossil taxa. In contrast, the Cp samples of the species of *Ginkgoites* have negative values against PC3. Thus, the compressions of *Ginkgoites tigrensis* and *G. skottsbergii* reveal the presence of aliphatic compounds with relatively short and branched chains and a high content of C=C bonds of aromatic compounds. In comparison, the compressions of the taxa of the Springhill Formation show an intermediate situation between *P. ornata*-*S. tigrensis* and *Ginkgoites* taxa. Despite this, most of the *Ptilophyllum micropapillosum* and *Ruflorinia orlandoi* Cp samples have negative values against PC3 reflecting an increase in carbonyl/carboxyl groups in regard to aromatic carbon groups (C=O/C=C).

Cretaceous gymnosperm fossil taxa regarding coal macerals and kerogen types. The 'A' Factor vs. 'C' Factor plot indicates the similarities between the kerogen types and coal maceral groups (Fig. 7). The foliar remains of *Pseudoctenis ornata* and *Squamastrobus tigrensis* have a general chemical composition similar to those of type I-II kerogen. In turn, the *Ginkgoites tigrensis* materials and most of those of *Ruflorinia orlandoi* and *Ptilophyllum micropapillosum* chemically resemble a type II kerogen composition. Thus, most fossil taxa are characterized by a medium to high content of aliphatic groups ('A' Factor) and a variable contribution of oxygen-containing compounds ('C' Factor), adopting a similar chemical composition to the liptinite maceral group (derived from the decomposition

of algae, bacteria, and zooplankton and cuticles, spores, and resins). On the other hand, the compression of *G. skottsbergii* has a chemical composition similar to type III kerogen which is mainly characterized by a low content of aliphatic groups.

Particularly, the compressions of *Ruflorinia orlandoi* and *Ptilophyllum micropapillosum* have medium to high values for 'A' Factor and medium values for 'C' Factor which are similar to the values obtained for some samples of sporinite, cutinite, and resinite (Fig. 7). Cuticle samples from both taxa show great variability, mainly in the relative contribution of oxygen-containing compounds (carbonyl/carboxyl groups).

The values of 'A' and 'C' Factors obtained for the Ct samples of *Squamastrobus tigrensis* and *Pseudoctenis ornata* are very high and similar to those of the compressions from which are derived. Thus, the *S. tigrensis* and *P. ornata* specimens are, regardless of the sample forms (Cp and Ct), chemically similar to the bituminite (T) samples belonging to the liptinite maceral group. In the case of *Ginkgoites tigrensis*, both Cp and Ct samples have low to medium values for 'C' Factor and medium to high values for 'A' Factor. Thus, *G. tigrensis* partially resembles the chemistry of cutinite, resinite, and sporinite macerals (liptinite group macerals). On the other hand, the *G. skottsbergii* Cp sample is chemically similar to the vitrinite maceral (Fig. 7).

DISCUSIONS

FTIR spectroscopy chemical characterization

For all fossil taxa, the PCA results indicate the existence of a certain degree of interspecific and intraspecific variability. Cuticular characteristics (such as papillae, hairs, cuticular striations, etc.) and chemical compositions of geopolymers derived from cutins and/or cutans (highly variable), as well as from other minor constituents, could contribute to chemical variability of the cuticles of the analyzed taxa (Lafuente Diaz et al., 2020a). In turn, variability (intra- and interspecific) could also be intensified or not, depending on the diagenetic processes that alter the original chemistry of the plant organic matter (Lafuente Diaz et al., 2020b).

The chemical composition of the fossil taxa from the Springhill Formation was evaluated considering the different frond parts. In the case of *Ptilophyllum micropapillosum*, the sampling differentiated among apical, middle, and basal zones. However, in this bennettitalean, a distinctive pattern distinguishing the frond parts is absent. Consequently, a gradual chemical transition in the composition of the leaf tissues towards those of the rachis is considered (Lafuente Diaz et al., 2019a). Also, the *Ruflorinia orlandoi* fronds were analyzed considering pinnules and rachis differentially. For each specimen of this fossil species, the rachis have a higher content of C=C bonds than the pinnae. The latter would probably be due to the transformation of more developed lignified tissue (i.e., supporting and conducting tissues) in the rachis than in the pinnae (Lafuente Diaz et al., 2020a).

In *Ruflorinia orlandoi* and *Ptilophyllum micropapillosum*, the cuticles have a higher content of aromatics than their corresponding compressions. Thus, the Ct samples of both fossil species have an aliphatic composition that is complemented by a relatively high proportion of aromatic compounds (C=C cont and C-H aromatic out-of-plane bending vibrations) (Lafuente Diaz et al., 2019a, 2020a). These cuticles probably contain a higher proportion of phenylpropanoids and aromatic domains in cutins and cutans, respectively (e.g., Villena et al., 1999; Deshmukh et al., 2005; Fich et al, 2016). Furthermore, the presence of other phenolic compounds, which could potentially compose the cuticles, would increase the *R. orlandoi* and *P. micropapillosum* cuticular aromaticity. In turn, the cuticles of both fossil taxa would be composed of polymeric structures with a relatively low degree of cross-linking (i.e., high CHal/C=O values). This dynamic could be the result of the rupture of ester bonds in cuticular biomacropolymers (e.g., cutins and cutans) implying a lower degree of polymeric cross-linking (Lafuente Diaz et al., 2019a, 2020a).

In Cp samples of the Carboniferous fossil taxa from the Northern Hemisphere, the relatively high values of the C=C cont ratio (with respect to the cuticles) were considered as derived from the organic compounds present in the preserved mesophyll between both epidermises (Zodrow et al., 2009, among others). In the cases of *Squamastrobus tigrensis* and *Pseudoctenis ornata*, the relatively high values of C=C cont in the Cp samples would

445 be the result of the occurrence of lignified tissues in the vascular bundles as well as in the
446 sclerenchyma fibers of the hypodermis remains (see Fig. 4) (Lafuente Diaz, 2019; Lafuente
447 Diaz et al., 2018). In the *P. ornata* samples, which have the most aliphatic compressions, it
448 is possible that the cuticular membranes and the mesophyll have been mainly constituted
449 by aliphatic compounds with long and unbranched chains. Most likely, during the
450 fossilization process, the chemical composition of the *P. ornata* mesophyll was differentially
451 altered (Lafuente Diaz et al., 2020b).
452 The compressions of *Squamastrobus tigrensis*, *Pseudoctenis ornata*, and
453 *Ginkgoites tigrensis* have a high degree of similarity with their respective cuticles. This fact
454 is interpreted as the result of a natural oxidation process which the foliar remains of each
455 taxon have undergone, to a certain degree, during diagenesis and/or post-diagenesis. The
456 probable natural oxidation of the compressions would have been a consequence of
457 particular geophysicochemical conditions due to the recurrent volcanic activity during the
458 sedimentation of the Baqueró Group. Thus, the interaction between the plant remains and
459 the volcanic ash, which covered them at the time of their deposition and during the
460 fossilization process, would originate variably oxidized compressions due to the fluctuant
461 intensity of volcanism according to the formations and fossil levels. Accordingly, a probable
462 preservation model that considers the peculiarities of the fossil taxa from the Baqueró
463 Group as well as the key role of volcanic activity in the fossilization process was proposed
464 by Lafuente Diaz et al. (2018, 2020b).
465 The aromaticity of the two ginkgoalean fossil species, *Ginkgoites tigrensis* and *G.*
466 *skottsbergii*, is particularly relevant. The Cp sample of *G. skottsbergii* is the compression
467 with the highest aromaticity of the entire set of studied fossil taxa. For the interpretation of
468 the data of the genus *Ginkgoites*, the chemical knowledge of the leaves of *Ginkgo biloba*,
469 the unique extant representative of this plant group (Ginkgoales), was considered. Thus, for
470 *G. tigrensis* and *G. skottsbergii*, it is probable that the presence of lignin in the vascular
471 bundles and of other phenolic compounds (i.e., flavonoids, tannins, and phenolic lipids such
472 as anacardic acids and cardanols) is responsible for the high contribution of aromatic

structures in the mesophyll of these two fossil taxa (Biswas and Jori, 1997; Brillouet et al., 2013, 2014; Chamberlain, 1965; Duarte et al., 2013; Lafuente Diaz et al., 2019b; Yoshitama, 1997).

The two species of *Ginkgoites* were collected in fossiliferous levels that have notable differences both in lithology and in the palaeoenvironmental conditions. Particularly, the *G. tigrensis* specimens (BTG fossiliferous level, Anfiteatro de Ticó Formation), preserved in volcanic tuff, would have undergone a natural oxidation process mainly due to the interaction of plant remains with cold volcanic ash (Lafuente Diaz et al., 2020b). In contrast, *G. skottsbergii*, preserved in sandstones without evidence of volcanic influence, is the less aliphatic compression (lowest CHal/C=C and 'A' Factor values) of the entire fossil taxa. On the other hand, the relatively high contribution of aromatic compounds (C=C cont) in the Ct sample of *G. tigrensis* (Ct4) is probably related to the chemical composition of the two main constituent biomacropolymers of the cuticle (cutins and cutans), as is the case with the fossil taxa from the Springhill Formation. The presence of adequate proportions of phenylpropanoids and aromatic domains in cutins and cutans would have been responsible for the occurrence in the cuticle of *G. tigrensis* of a strong aromatic signal in addition to an aliphatic character (Lafuente Diaz et al., 2020b).

Cretaceous gymnosperm fossil taxa from Argentina: chemical preservation types

Most of foliar compressions of the Cretaceous gymnosperms from the Santa Cruz province here analyzed have a distinctive chemical composition regarding preservation types. Thus, compressions differ chemically from other taxa from the Northern Hemisphere previously studied and, therefore, do not fully conform to the three best-known plant fossils preservation types. They are the so-called cuticle-free coalified layers fossilized cuticles, and compressions that were proposed by Zodrow and Mastalerz (2009) and Zodrow et al. (2009) (Table 5).

The foliar compressions of the Patagonian fossil taxa differ from the cuticle-free coalified layers due to the presence of the adaxial and abaxial epidermises. In turn, the fossilized cuticles are characterized by a general poor preservation of the epidermal features. This is not the case with the fossil taxa studied here where the epidermises show very well preserved cuticular features such as anticlinal and periclinal walls, papillae and/or hair, and subsidiary and guard cells (Fig. 4).

On the other hand, the main difference that the Patagonian material exhibits with the compression preservation type is the transformation of the mesophyll, through geological time and diverse geophysicochemical reactions, into a maceral group different from the vitrinite. Thus, the compressions of *Squamastrobus tigrensis*, *Pseudoctenis ornata*, and *Ginkgoites tigrensis* (Baqueró Group) as well as those of *Ptillophyllum micropapillosum* and *Ruflorinia orlandoi* (Springhill Formation) are chemically similar to the liptinite maceral group (sporinite, cutinite, resinite, bituminite; Fig. 7). This fact differs from the spectroscopically analyzed Carboniferous compressions of Canada, which chemically resemble the vitrinite maceral group. Similarly, the foliar compression of *Ginkgoites skottsbergii* has a chemical composition analogous to that exhibited by the vitrinite maceral group.

Terminology applied to FTIR spectroscopy and Patagonian foliar compressions. From a paleobotanical point of view, all the studied fossil taxa consist of coalified compressions (e.g., Scott and Collinson, 1982). However, over time and the evolution of spectroscopic studies applied to paleobotany, several concepts have been created to reflect the particularities of plant fossil preservations regarding the FTIR chemical data (e.g., Zodrow and Mastalerz, 2009; Zodrow et al., 2009). As mentioned above, the best-known preservation types (i.e., compression, fossilized cuticle, and cuticle-free coalified layer) initially characterized fossil materials from the Carboniferous plants of the Northern Hemisphere. However, it is observed that the Patagonian fossil taxa herein analyzed show different preservation types.

The preservation types of the foliar remains of *Squamastrobus tigrensis* (Coniferales) and *Jonhstonia coriacea* (Corystospermales) were initially described as fossilized compressions (Lafuente Diaz et al. 2016, 2018). These studies indicated the existence of different geophysicochemical conditions, varying along a multidimensional continuum, which would have originated the different preservation types that could occur in nature. In turn, this interpretation comprises the probable infinity of intermediate stages that take place in the wide spectrum of transformations of the organic matter. From this idea, the need to evaluate a preservation type classification that is sufficiently broad to include the particularities of the different fossil taxa arises. These particularities should be addressed according to the botanical knowledge of the fossil species, the paleoenvironment, and other geophysicochemical conditions that could alter or preserve the original chemical composition of the plants. Thus, Lafuente Diaz et al. (2019a) proposed a new concept, i.e., liptinitic compression to define the preservation type of the Patagonian taxon *Ptillophyllum micropapillosum*. This concept, which reflects the chemical composition and similarity with the liptinite maceral group, can be extrapolated to other foliar compressions belonging to paleoflora that inhabited the Santa Cruz province.

According to the similarity of the foliar fossil remains with respect to the chemical composition of the macerals, the compressions of the Patagonian fossil taxa have been characterized by a new designation adding to the term *'compression'* an adjective that refers to one of the three maceral groups (Lafuente Diaz, 2019). This terminology allows extrapolating the preservation types (compression + maceral adjective) to diverse fossil taxa of different ages and lithologies.

Most compressions are named as liptinitic compressions, including the fossil remains of *Ruflorinia orlandoi*, *Pseudoctenis ornata*, *Ptilophyllum micropapillosum*, *Ginkgoites tigrensis*, and *Squamastrobus tigrensis* (Lafuente Diaz et al., 2018, 2019a, 2020a).

On the other hand, the *Ginkgoites skottsbergii* compression is chemically similar to the vitrinite maceral group and consequently called vitrinitic compression.

Thus, *G. skottsbergii* is the only analyzed fossil taxon that agrees with the compression definition which was proposed from FTIR studies carried out on plant fossil remains from the Carboniferous of the Northern Hemisphere (Zodrow and Mastalerz, 2009; Zodrow et al., 2009). Consequently, the *G. skottsbergii* preservation type, from the spectroscopic point of view, is similar to that of *Alethopteris ambigua*, *A. pseudograndinioides*, *Cordadites principales, Dicroidium odontopteroides*, *Johnstonia coriacea*, *Kurtziana* sp., *Macroneuropteris scheuchzeii*, among others (D'Angelo, 2006; D'Angelo et al., 2010; Zodrow et al., 2010; D'Angelo et al., 2011; Zodrow et al., 2012).

CONCLUSIONS

In this contribution, comparative semi-quantitative FTIR spectroscopy studies among different plant fossil taxa from the Santa Cruz province are presented, considering the diversity existing in the plant communities during the Lower Cretaceous in Patagonia. The most important conclusions are summarized as follows:

1) In the foliar plant fossil remains, the preserved chemistry is the result in part of the original chemistry of the plants (i.e., structural organic constituents), and partially due to different modifications introduced during the fossilization process.

2) The PCA results indicate the existence of a certain degree of inter- and intraspecific variability. The former would be attributable to structural differences among the plant groups and the constituents making up the leaf types from which the foliar compressions derive. In contrast, the intraspecific variability, specifically relevant in Ct samples, is related to the cuticular features (i.e., presence of papillae, hairs, cuticular striations, among others), and the variable chemical compositions of the biomacropolymers (cutins and cutans) that compose the cuticle. Additionally, the diagenetic processes would alter the original chemistry of organic matter and thus they contribute to the intra- and interspecific variability.

3) The chemical composition of the Cretaceous cuticles from Patagonia is remarkably distinctive with respect to other previously analyzed cuticles from the Carboniferous of the Northern Hemisphere and the Triassic of Argentina.

3. a) In the cases of *Ptylophyllum micropapillosum* and *Ruflornia orlandoi* (Springhill Formation), a significant contribution of aromatic functional groups probably forming part of the structural components of cuticles such as cutins, cutans, and phenolic compounds (e.g., lignins) is observed.

3. b) For the fossil taxa from the Baqueró Group, the similarity between the Cp and Ct samples in each fossil taxon is most likely the result of a natural oxidation process which the foliar remains had undergone during diagenesis and/or post-diagenesis. Thus, a preponderant role in the volcanic activity in the fossilization processes of *Pseudoctenis ornata*, *Ginkgoites tigrensis*, and *Squamastrobus tigrensis* is suggested.

3. c) In the *Ginkgoites tigrensis* and *G. skottsbergii* samples, the presence of aromatic compounds is particularly relevant. The aromaticity of these species of *Ginkgoites* could be due to the contribution of the aromatic structures that compose the mesophyll tissues. These aromatic structures most probably derive from phenolic compounds, as it occurs in the unique extant representative of the Ginkgoales, that is, *Ginkgo biloba*. The strong aromatic signature of the *Ginkgoites tigrensis* cuticle distinguishes this taxon from the other gymnosperms analyzed (*Dicroidium* flora and Medullosales), whereas *G. tigrensis* resembles those of *Ruflorinia orlandoi* and *Ptillophyllum micropapillosum*.

4) The FTIR results indicate the necessity to use specific terminology to describe adequately the foliar compressions from the Lower Cretaceous of the Santa Cruz province. For this, the exhibited preservation types are considered in relation to the similarity of the foliar compression with the maceral groups. Thus, the new terms referring to liptinitic, vitrinic, or inertinitic compressions are proposed. The compressions of most of the fossil taxa analyzed (*Pseudoctenis ornata*, *Ginkgoites tigrensis, Squamastrobus tigrensis, Ptilophyllum micropapillosum*, and *Ruflorinia orlandoi*) are defined as liptinitic compressions

due to the chemical similarity with the chemistry of the liptinite maceral group (derived from the decomposition of algae, bacteria, and zooplankton, cuticles, spores, and resins) and the considered spectroscopic data of two PCA variables (i.e., 'A' and 'C' Factors). The case of *Ginkgoites skottsbergii* is particular, which is chemically similar to the vitrinite maceral group (derived from lignin and tannin of vascular plants); consequently, its preservation type is called vitrinitic compression.

The spectroscopic analysis carried out on the Cretaceous plant remains of Argentina allows characterizing the preserved chemical composition of fossil taxa belonging to different systematic groups. Thus, the more chemical information is revealed from the fossil plants, the more comprehensive knowledge will be acquired about the plant communities that inhabited during the Lower Cretaceous of the Santa Cruz province.

Acknowledgments

We dedicate this article to Edith L. Taylor for always being an advocate for women in science and her stimulating papers and books in paleobotany. This contribution was partially supported by the Consejo Nacional de Investigaciones Científicas y Técnicas (CONICET) and the Agencia Nacional de Promoción Científica y Tecnológica (ANPCyT) through the following grants: CONICET PIP 2012/12, CONICET PUE 2016/0098 and ANPCyT PICT 2012/528 and 2015-2206. Orlando Cárdenas is grateful for his technical assistance to obtain cuticle samples for morpho-anatomical studies, and Cp and Ct samples for FTIR spectroscopy. We thank Gerardo Camí, Instituto IQUIR-CONICET-UNR (www.iquir-conicet.gov.ar) and the Instituto CEQUINOR-CONICET (www.cequinor.conicet.gob.ar) for the FTIR spectra acquisition.

References

Aguirre-Urreta MB 2002 Invertebrados del Cretácico Inferior. Pages 439–459 in MJ Haller, ed. Geología y Recursos Naturales de Santa Cruz. Congr Geol Argent. Calafate, Buenos Aires.

Archangelsky A, RR Andreis, S Archangelsky, A Artabe 1995 Cuticular characters adapted to volcanic stress in a new Cretaceous cycad leaf from Patagonia, Argentina. Considerations on the stratigraphy and depositional history of the Baqueró Formation. Rev Palaeobot Palynol 89:213–233.

Archangelsky S 1965 Fossil Ginkgoales from the Ticó flora, Santa Cruz Province, Argentina. Bull Br Mus Nat Hist Geol 10:119–137.

Archangelsky S 2003 Flora Cretácica del Grupo Baqueró. Monografías del Museo Argentino de Ciencias Naturales “Bernardino Rivadavia”, no. 4.

Archangelsky S, GM Del Fueyo 1989 *Squamastrobus* gen n., a fertile podocarp from the early Cretaceous of Patagonia, Argentina. Rev Palaeobot Palynol 59:109–126.

Archangelsky S, A Archangelsky, G Cladera 2012 Palinología y paleoambientes en el perfil de Bajo Comisión (Cretácico), provincia de Santa Cruz, Argentina. Rev Mus Argent Cs Nat, NS,14:23–39.

Barreda V, S Archangelsky 2006 The southernmost record of tropical pollen grains in the Cretaceous of Patagonia, Argentina. Cretac Res 27:778–787.

Benítez J, AJ Matas, A Heredia 2004 Molecular characterization of the plant biopolymer cutin by AFM and spectroscopic techniques. J struct biol 147:179–184.

Biswas V, BM Johri 1997 Ginkgoales. Pages 98–126 in V Biswas, BM Johri, eds. The Gymnosperms. Springer, New York.

Brillouet JM, C Romieu, B Schoefs, K Solymosi, V Cheynier, H Fulcrand, JL Verdeil, G Conéjéro 2013 The tannosome is an organelle forming condensed tannins in the chlorophyllous organs of Tracheophyta. Ann Bot 112:1003–1014.

662 Brillouet JM, C Romieu, M Lartaud, E Jublanc, L Torregrosa, C Cazevieille 2014 Formation
663 of vacuolar tannin deposits in the chlorophyllous organs of Tracheophyta: from
664 shuttles to accretions. Protoplasma 251:1387–1393.
665 Carrizo MA, GM Del Fueyo 2015 The Early Cretaceous Megaflora of the Springhill
666 Formation, Patagonia. Paleofloristic and Paleonvironmental Inferences. Cretac Res
667 56:93–109.
668 Carrizo MA, GM Del Fueyo, F Medina 2014 Foliar cuticle of *Ruflorinia orlandoi* nov. sp.
669 (Pteridospermophyta) from the Lower Cretaceous of Patagonia. Geobios 47:87–99.
670 Carrizo MA, MA Lafuente Diaz, GM Del Fueyo, G Guignard 2019 Cuticle ultrastructure in
671 *Brachyphyllum garciarum* sp. nov (Lower Cretaceous, Argentina) reveals its
672 araucarian affinity. Rev Palaeobot Palynol 269:104–128.
673 Césari SN, CO Limarino, M Llorens, MG Passalía, VS Perez Loinaze, EI Vera 2011 High-
674 precision late Aptian U/Pb age for the Punta del Barco Formation (Baqueró Group),
675 Santa Cruz Province, Argentina. J S Am Earth Sci 31: 426–431.
676 Chamberlain CJ 1965 Gymnosperms. Structure and evolution. University of Chicago Press,
677 Chicago-Illinois.
678 Cladera G, R Andreis, S Archangelsky, R Cúneo 2002 Estratigrafía del Grupo Baqueró,
679 Patagonia (Provincia de Santa Cruz, Argentina). Ameghiniana 39:3–20.
680 Colthup NB, LH Daly, SE Wiberley 1990 Introduction to Infrared and Raman Spectroscopy.
681 Academic Press, New York.
682 D'Angelo JA 2006 Analysis by Fourier transform infrared spectroscopy of *Johnstonia*
683 (Corystospermales, Corystospermaceae) cuticles and compressions from the
684 Triassic of Cacheuta, Mendoza, Argentina. Ameghiniana 43:669–685.
685 D'Angelo JA 2019 Molecular structure of the cuticles of *Dicroidium* and *Johnstonia*
686 (Corystospermaceae, Triassic, Argentina). Ecophysiological adaptations of two
687 chemically indistinguishable, morphology-based taxa. Rev Palaeobot Palynol
688 268:109–124.

D’Angelo JA, EL Zodrow 2015 Chemometric study of structural groups in medullosalean foliage (Carboniferous, fossil Lagerstätte, Canada): Chemotaxonomic implications. Int J Coal Geol 138:42–54.

D'Angelo JA, EL Zodrow 2016 3D chemical map and a theoretical life model for *Neuropteris ovata* var. *simonii* (index fossil, Asturian, Late Pennsylvanian, Canada). Int J Coal Geol 153:12–27.

D'Angelo JA, EL Zodrow 2018a Density and biomechanical properties of fossil fronds. A case study of *Neuropteris ovata* (seed fern, Late Pennsylvanian, Canada). Int J Coal Geol 198:63–76.

D’Angelo JA, EL Zodrow 2018b Fossil cutin of *Johnstonia coriacea* (Corystospermaceae, Upper Triassic, Cacheuta, Argentina). Int J Coal Geol 189:70–74.

D’Angelo JA, EL Zodrow, A Camargo 2010 Chemometric study of functional groups in Pennsylvanian gymnosperm plant organs (Sydney Coalfield, Canada): implications for chemotaxonomy and assessment of kerogen formation. Org Geochem 41:1312–1325.

D’Angelo JA, LB Escudero, W Volkheimer, EL Zodrow 2011 Chemometric analysis of functional groups in fossil remains of the *Dicroidium* flora (Cacheuta, Mendoza, Argentina): implications for kerogen formation. Int J Coal Geol 87:97–111.

D'Angelo JA, PC Lyons, M Mastalerz, EL Zodrow 2013 Fossil cutin of *Macroneuropteris scheuchzeri* (Late Pennsylvanian seed fern, Canada). Int J Coal Geol 105:137–140.

Del Fueyo GM, L Villar de Seoane, A Archangelsky, V Guler, M Llorens, S Archangelsky, JC Gamerro, E Musacchio, M Passalia, V Barreda 2007 Biodiversidad de las Paleofloras de Patagonia Austral durante el Cretácico Inferior. Pages 101–122 in S Archangelsky, T Sánchez, EP Tonni, eds. Ameghiniana SP Vol 11. Asociación Argentina Paleontológica, Buenos Aires.

Del Fueyo GM, S Archangelsky, M Llorens, R Cúneo 2008 Coniferous ovulate cones from the lower Cretaceous of Santa Cruz province, Argentina. Int J Plant Sci 169:799–813.

717 Deshmukh AP, AJ Simpson, CM Hadad, PG Hatcher 2005 Insights into the structure of
718 cutin and cutan from *Agave americana* leaf cuticle using HRMAS NMR
719 spectroscopy. Org Geochem 36:1072–1085.
720 Duarte MR, DC Souza, RE Costa 2013 Comparative Microscopic Characters of *Ginkgo*
721 *biloba* L. from South America and Asia. Lat Am J Pharm 32:1118–23.
722 Fich EA, NA Segerson, JK Rose 2016 The plant polyester cutin: biosynthesis, structure,
723 and biological roles. Annu Rev Plant Biol 67:207–233.
724 Ganz H, W Kalkreuth 1987 Application of infrared spectroscopy to the classification of
725 kerogen-types and the evolution of source rock and oil-shale potentials. Fuel
726 66:708–711.
727 Guignard G, GM Del Fueyo, L Villar de Seoane, MA Carrizo, MA Lafuente Diaz 2016.
728 Insights into the leaf cuticle fine structure of *Ginkgoites skottsbergii* Lund. from the
729 Albian of Patagonia and its relationship within Ginkgoaceae. Rev Palaeobot. Palynol
730 232: 22–39.
731 Guler MV, S Archangelsky 2006 Albian dinoflagellate cysts from the Kachaike Formation,
732 Austral Basin, Southwest Argentina. Rev Mus Argent Cs Nat, NS, 8:179–184.
733 Guo Y, RM Bustin 1998 Micro-FTIR spectroscopy of liptinite macerals in coal. Int J Coal
734 Geol 36:259–275.
735 Ingle JD, SR Crouch 1988 Spectrochemical Analysis. Prentice-Hall, New Jersey.
736 Izenman AJ 2008 Modern Multivariate Statistical Techniques: Regression, Classification,
737 and Manifold Learning (Springer Texts in Statistics). Springer, New York.
738 Jolliffe IT 2002 Principal Component Analysis. Springer, New York.
739 Lafuente Diaz MA, JA D'Angelo, GM Del Fueyo 2015.Chemical characterization of
740 Podocarpaceae leaves from Early Cretaceous of Patagonia. Ameghiniana 52(4): 38-
741 39.
742 Lafuente Diaz MA, JA D'Angelo, GM Del Fueyo 2016 Chemical preservation states of
743 Mesozoic gymnosperms leaves (Santa Cruz and Mendoza, Argentina). A
744 chemometric approach. Bol Asoc Latinoamer Paleobot Palin 16:159.

745 Lafuente Diaz M A, JA D'Angelo, GM Del Fueyo, MA Carrizo 2017 Chemical
746 characterization of Pteridospermophyta fronds from the Lower Cretaceous of
747 Patagonia. Resúmenes RC Asoc Paleont Argent 2017: 44
748 Lafuente Diaz MA, JA D'Angelo, GM Del Fueyo, EL Zodrow 2018a Fossilization model for
749 *Squamastrobus tigrensis* foliage in a volcanic-ash deposit: implications for
750 preservation and taphonomy (Podocarpaceae, Lower Cretaceous, Argentina).
751 Palaios 33:323–337.
752 Lafuente Diaz MA, JA D'Angelo, GM Del Fueyo, MA Carrizo 2018b Chemical preservation
753 of Cretaceous gymnosperms leaves from the Baqueró Group (Aptian, Santa Cruz,
754 Argentina). Bol Asoc Latinoamer Paleobot Palin 18:59–60
755 Lafuente Diaz MA, MA Carrizo, GM Del Fueyo, JA D'Angelo 2018c Preserved chemistry of
756 *Ptilophyllum* fronds from the Springhill Formation (Lower Cretaceous, Argentina).
757 Resúmenes RC Asoc Paleont Argent 2018:70.
758 Lafuente Diaz MA, MA Carrizo, GM Del Fueyo, JA D'Angelo 2019a Chemometric approach
759 to the foliar cuticle of *Ptilophyllum micropapillosum* sp. nov. from the Springhill
760 Formation (Lower Cretaceous, Argentina): Rev Palaeobot Palynol 271:104110.
761 Lafuente Diaz MA, JA D'Angelo, GM Del Fueyo, MA Carrizo 2019b Chemical
762 characterization of *Ginkgoites* Seward leaves from the Lower Cretaceous of
763 Patagonia (Santa Cruz province, Argentina). Resúmenes RC Asoc Paleont Argent
764 2019:57.
765 Lafuente Diaz MA, JA D'Angelo, GM Del Fueyo, MA Carrizo 2020a FTIR spectroscopic
766 features of the pteridosperm *Ruflorinia orlandoi* and host rock (Springhill Formation,
767 Lower Cretaceous, Argentina). J S Am Earth Sci 99:102520.
768 Lafuente Diaz MA, GM Del Fueyo, JA D'Angelo, MA Carrizo 2020b Preserved chemistry of
769 Cretaceous gymnosperm leaves in volcanic-ash deposits. Cretac Res 2020,
770 104646.

771 Limarino CO, MG Passalia, M Llorens, EI Vera, VS Perez Loinaze, SN Césari 2012
772 Depositional environments and vegetation of Aptian sequences affected by
773 volcanism in Patagonia. Palaeogeogr Palaeoclimatol Palaeoecol 323:22–41.
774 Lin R, GP Ritz 1993a Reflectance FT-IR microspectroscopy of fossil algae contained in
775 organic-rich shale. Appl Spectrosc 47: 265–271.
776 Lin R, GP Ritz 1993b. Studying individual macerals using IR microspectroscopy, and
777 implications on oil versus gas/condensate proneness and “low-rank” generation. Org
778 Geochem 20: 695–706.
779 Llorens M, VS Perez Loinaze, MG Passalia, EI Vera 2020 Palynological, megafloral and
780 mesofossil record from the Bajo Grande area (Anfiteatro de Ticó Formation,
781 Baqueró Group, Upper Aptian), Patagonia, Argentina. Rev Palaeobot Palynol
782 273:104137.
783 Lundblad B 1971. A restudy of the ginkgoalean leaves of the Mesozoic flora of Lago San
784 Martin, Patagonia (*Ginkgoites skottsbergii*-n.sp.). J Indian Bot Soc 50A: 236–241.
785 Mastalerz M, RM Bustin 1996 Application of reflectance micro-Fourier Transform infrared
786 analysis to the study of coal macerals: an example from the Late Jurassic to Early
787 Cretaceous coals of the Mist Mountain Formation, British Columbia, Canada. Int J
788 Coal Geol 32:55–67.
789 Mastalerz M, RM Bustin 1997 Variation in chemistry of macerals in coals of the Mist
790 Mountain Formation, Elk Valley coalfield, British Columbia, Canada. Int J Coal Geol
791 33:43–59.
792 Matsumura WMK, NM Balzaretti, R Iannuzzi 2016 Fourier Transform Infrared
793 characterization of the Middle Devonian non-vascular plant *Spongiophyton*.
794 Palaeontology 59: 365–386.
795 Ottone EG, MB Aguirre-Urreta 2000 Palinomorfos cretácicos de la Formación Springhill en
796 Estancia El Salitral, Patagonia Austral, Argentina. Ameghiniana 37:379–382.
797 Perez Loinaze VS, EI Vera, MG Passalia, M Llorens, R Friedman, CO Limarino, SN Césari
798 2013 High-precision U-Pb zircon age from the Anfiteatro de Ticó Formation:

Implications for the timing of the early angiosperm diversification in Patagonia. J S Am Earth Sci 48:97–105.

Petersen HI, HP Nytoft 2006 Oil generation capacity of coals as a function of coal age and aliphatic structure. Org Geochem 37: 558–583.

Pšenička J, EL Zodrow, M Mastalerz, J Bek 2005 Functional groups of fossil marattialeans: chemotaxonomic implications for Pennsylvanian tree ferns and pteridophylls. Int J Coal Geol 61:259–280.

Riccardi AC 1971 Estratigrafía en el oriente de la Bahía de la Lancha, Lago San Martín, Santa Cruz, Argentina. Rev Mus La Plata, NS, Geol 7:245–318.

Riccardi AC 1988 The Cretaceous system of southern South America. Geol Soc Am Mem 168.

Riccardi AC, CA Gulisano, J Mojica, O Palacios, C Schubert, MRA Thomson 1992 Western South America and Antarctica. Pages 122–161 in GEG Westermann, ed. The Jurassic of the Circum-Pacific. Cambridge University Press.

Scott A, M Collinson 1982 Investigationg fossil plant beds Part 1: the origin of fossil plats and their sediments. Geol teach 7(4):114–122

Thomas CR 1949 Manantiales Field, Magallanes Province, Chile. AAPG Bulletin 33:1579–1589.

Villar de Seoane L, S Archangelsky 2008 Taxonomy and biostratigraphy of Cretaceous megaspores from Patagonia, Argentina. Cretac Res 29:354–372.

Villena JF, E Domínguez, D Stewart, A Heredia 1999 Characterization and biosynthesis of non-degradable polymers in plant cuticles. Planta 208:181–187.

Wang SH, PR Griffiths 1985 Resolution enhancement of diffuse reflectance IR spectra of coals by Fourier self-deconvolution. 1. C-H stretching and bending modes. Fuel 64:229–236.

Yoshitama K 1997 Flavonoids of *Ginkgo biloba*. Pages 287–300 in T Hori, RW Ridge, W Tulecke, P Del Tredici, J Trémouillaux-Guiller, H Tobe, eds. *Ginkgo biloba* a global treasure, from biology to medicine. Springer, Tokio.

827 Zodrow EL, M Mastalerz 2001 Chemotaxonomy for naturally macerated tree-fern cuticles
828 (Medullosales and Marattiales), Carboniferous Sydney and Mabou Sub-basins,
829 Nova Scotia, Canada. Int J Coal Geol 47: 255–275.
830 Zodrow EL, M Mastalerz 2009 A proposed origin for fossilized Pennsylvanian plant cuticles
831 by pyrite oxidation (Sydney Coalfield, Nova Scotia, Canada). Bull Geosci 84:227–
832 240.
833 Zodrow EL, M Mastalerz 2019 Novel preservation state of *Dolerotheca* (medullosalean
834 male organ) from the Late Pennsylvanian of the Sydney Coalfield, Nova Scotia,
835 Canada. Atl Geol 55:251–263.
836 Zodrow EL, JA D'Angelo, M Mastalerz, D Keefe 2009 Compression-cuticle of seed ferns:
837 Insights from liquid–solid states FTIR (Late Palaeozoic-Early Mesozoic, Canada-
838 Spain-Argentina). Int J Coal Geol 79:61–73.
839 Zodrow EL, JA D'Angelo, M Mastalerz, CJ Cleal, D Keefe 2010 Phytochemistry of the
840 fossilized-cuticle frond *Macroneuropteris macrophylla* (Pennsylvanian seed fern,
841 Canada*).* Int J Coal Geol 84:71–82.
842 Zodrow EL, JA D'Angelo, R Helleur, Z Šimůnek 2012 Functional groups and common
843 pyrolysate products of *Odontopteris cantabrica* (index fossil for the Cantabrian
844 Substage, Carboniferous). Int J Coal Geol 100:40–50.
845 Zodrow EL, R Helleur, U Werner-Zwanziger, B Chen, JA D'Angelo 2013 Spectrochemical
846 study of coalified *Trigonocarpus grandis* (Pennsylvanian tree-fern ovule, Canada):
847 Implications for fossil–organ linkage. Int J Coal Geol 109:24–35.
848 Zodrow EL, JA D'Angelo, WA Taylor, T Catelani, JA Heredia-Guerrero, M Mastalerz 2016
849 Secretory organs: Implications for lipoid taxonomy and kerogen formation (Seed
850 ferns, Pennsylvanian, Canada). Int J Coal Geol 167:184–200.
851 Zodrow EL, JA D'Angelo, CJ Cleal 2017 3D chemometric model and frond architecture of
852 *Alethopteris ambigua* (Medullosales): Implications for reconstruction and taxonomy.
853 Palaeontogr Abt B 29:91–133.
854

855 Figure captions

856 **Figure 1.** Location map of the fossiliferous localities: Bajo Tigre and Punta del
857 Barco (1), Río Correntoso (2), and Bajo Comisión (3), Santa Cruz province, Argentina. The
858 numbers are related to the Lower Cretaceous formations from which each fossil taxon
859 studied was collected.

860 **Figure 2.** FTIR sample forms. **A-D.** *Pseudoctenis ornata*. (Cycadales). **A-B.** BA Pb
861 1222. **A.** Rock sample with a frond fragment. **B.** Detail of the foliar compression released
862 from the rock matrix. **C-D.** Chemical treatment and resulting sample forms, BA Pb 1217. **C.**
863 Compression (Cp) obtained after steps 1st, 2nd, and 3rd. **D.** Cuticle (Ct) obtained after
864 steps 1st, 2nd, 3rd, and 4th.

865 **Figure 3.** Typical functional groups at different wavenumbers, in a model spectrum
866 based on plant fossil (foliar compression).

867 **Figure 4.** Foliar epidermises under SEM. **A.** *Pseudoctenis ornata*. **1.** Adaxial
868 epidermis internal view, BA Pb MEB 645. **2.** Abaxial epidermis external view. Papillae in
869 ordinary epidermal cells and subsidiary cells, BA Pb MEB 646. **3.** Stomatal apparatus, detail
870 of the form and arrangement of papillae. Note geminated papilla (arrow), BA Pb MEB 643.
871 **B.** *Ginkgoites tigrensis*. Abaxial epidermis, BA Pb 589. **1.** Stomatal apparatuses in internal
872 view. **2 .** External view of stomatal apparatuses showing sunken guard cells. **3.** Detail
873 stomatal apparatus in internal view. **C.** *Squamastrobus tigrensis*. Abaxial epidermis, BA Pb
874 MEB 585. **1.** External view. Note anticlinal walls thickness. **2-3.** Internal view. **2.** Longitudinal
875 rows of stomatal apparatuses.**3.** Detail stomatal apparatus. Note hypodermic cell remains
876 (arrow). **D.** *Ruflorinia orlandoi*, external view. **1.** Rachis and pinnae with both epidermises
877 preserved, MPM Pb 15313. **2.** Stomatal apparatuses in groups, subsidiary cells with
878 striated simple, cuticular striations, MPM Pb 15329. **3.** Trichomes. Note bifurcated hair
879 (arrow), MPM Pb 15313. **E.** *Ptilophyllum micropapillosum,* MPM Pb 15355. **1.** Internal
880 view. Note parallel venation. **2.** External view. Small, simple papillae on ordinary
881 epidermal cells and subsidiary cells and, big, simple papillae (arrows) on veins. **3.**
882 Stomatal apparatus with two subsidiary cells. Note anticlinal walls sinuosity. **F.**

883 *Ginkgoites skottsbergii,* BA Pb MEB 249. **1.** Epidermis internal view. General aspect and
884 arrangement of stomatal apparatuses between veins. **2.** Rectangular ordinary epidermal
885 cells on veins. **3.** Stomatal apparatuses with guard cells preserved.
886 **Figure 5.** PCA (principal component analysis) plots from the six gymnosperms
887 analyzed. **A-C.** PC 1 vs. PC 2. **A-B.** Component loadings (area ratios). **A.** Full-scale. **B.**
888 Detail of the zone delimited in (A). **C-D.** Component scores. **C.** Individual samples of each
889 taxon are indicated. **D.** Simplified plot indicating the six fossil taxa (ellipses around the
890 groups have no statistical significance).
891 **Figure 6.** PCA (principal component analysis) plots from the six gymnosperms
892 analyzed. **A-C.** PC 1 vs. PC 3. **A-B.** Component loadings (area ratios). **A.** Full-scale. **B.**
893 Detail of the zone delimited in (A). **C-D.** Component scores. **C.** Individual samples of each
894 taxon are indicated. **D.** Simplified plot indicating the six fossil taxa (ellipses around the
895 groups have no statistical significance).
896 **Figure 7.** FTIR data (Cp and Ct), of the six Cretaceous gymnosperms of the Santa
897 Cruz province, plotted into the kerogen-type diagram. **A.** Full-scale diagram. **B.** Simplified
898 plot of (A) indicating approximate regions for different macerals (ellipses around the
899 groups have no statistical significance).
900
901 Table captions
902 **Table 1.** List of the six studied gymnosperms indicating the sampling used in each
903 of them and the corresponding reference.
904 **Table 2.** Wavenumber ranges in which main functional groups and classes of
905 compounds absorb.
906 **Table 3.** Definition of semi-quantitative area ratios derived from FTIR spectra.
907 **Table 4.** Morphological, anatomical, and ultrastructural characterization of the fossil
908 taxa spectroscopically studied.
909 **Table 5.** Terminology used to refer to chemical preservation types of plant fossils by
910 means of FTIR spectroscopy studies.

Appendix A

Supplementary data: FTIR spectra of the six Cretaceous gymnosperms fossil taxa from Argentina. Note Cp= compression (blue) and Ct= cuticle (red).

Appendix B

Supplementary data: Semi-quantitative FTIR data set of the six analyzed gymnosperms from the province of Santa Cruz, Argentina.

Appendix C

Supplementary data: Solution of principal component analysis (PCA).

Table 1. List of the six gymnosperms indicating the sampling used in each of them and corresponding references.

Fossil taxa	Foliar sampling		References
Ruflorinia orlandoi	Bipinnate frond	Pinnae and rachis	Lafuente Diaz et al., 2017, 2020a
Pseudoctenis ornata	Linear to acuminate pinnae		Lafuente Diaz et al., 2018b, 2020b
Ptilophyllum micropapillosum	Pinnate frond	Apical, middle, and basal frond parts	Lafuente Diaz et al., 2018c, 2019a
Ginkgoites tigrensis	Laminate divided into segments		Lafuente Diaz et al., 2019b, 2020b
Ginkgoites skottsbergii	Laminate divided into segments		Lafuente Diaz et al., 2019b
Squamastrobus tigrensis	Scale-like, adpressed and sessile		Lafuente Diaz et al., 2015, 2016, 2018a, 2018b, 2020b

Table 2. Wavenumber ranges in which main functional groups and classes of compounds absorb.

Range (cm^{-1})	Group and class of compound	Assignment
3450–3250	Hydroxyl (-OH) in alcohols and phenols	O–H stretch
2936–2913	Methylene and Methyl (CH_3-, CH_2-) in aliphatic compounds	CH_3–, CH_2– anti-symmetric stretch
2864–2843	CH_3–, CH_2– in aliphatic compounds	CH_3–, CH_2– symmetric stretch
1780-1720	C=O in γ-lactones, δ-lactones and aldehydes	C=O stretch
1724–1695	Carbonyl (C=O) in carboxylic acids, ketones	C=O stretch
1655-1580	C=O in β-keto esters and β-diketo esters	C=O stretch
1620–1498	Benzene ring in aromatic compounds	C=C aromatic ring stretch
1475–1450	CH_2 in aliphatic compounds	CH_2 bending (scissors) vibration
1465–1440	CH_3 in aliphatic compounds	Antisymmetric CH_3 deformation
~1410	CH-(CH_3) bond in aliphatic compounds	CH-(CH_3) symmetric deformation
1385–1375	CH_3 in aromatic and aliphatic compounds	CH_3–Ar, R symmetric deformation
1240–1070	C–O-C in ethers	C–O-C stretch
900–700	=CH in aromatic hydrocarbons	=C–H out-of-plane bending
730–720	CH_2 in long chain aliphatic compounds ($[CH_2]_n$, $n \geq 4$)	CH_2 rocking vibration

Table 3. Definition of semi-quantitative area ratios derived from FTIR spectra.

Ratio PCA variable	Band-region (cm^{-1}) Band-region ratios	Interpretation and remarks
CH_2/CH_3	3000-2800	Methylene/methyl ratio. It relates to the aliphatic chain length and degree of branching of aliphatic side groups (Lin and Ritz, 1993a, 1993b). Higher value implies comparatively longer and straight chains, a lower value shorter and more branched chains. Caution is advised using the ratio, as it may be misleading due to the contribution from CH_2 and CH_3 groups attached directly to aromatic rings (Petersen and Nytoft, 2006).
CHal/Ox	(3000-2800)/(1800-1600)	Aliphatic/oxygen-containing compounds ratio. Relative contribution of aliphatic CH stretching bands (CHal) to the combined contribution of oxygen-containing groups and aromatic carbon (Ox). From higher values decreasing oxygen-containing groups can be inferred, or the lower the CHal/Ox ratio, the higher the Ox term. This ratio could provide some information about oxidation in organic matter (e.g., Mastalerz and Bustin, 1997; Zodrow and Mastalerz, 2001).
C=O/C=C	(1700–1600)/(1600–1500)	Carbonyl/aromatic ratio of carbon groups. Relative contribution of C=O to aromatic carbon groups. Higher values indicate increasing carbonyl/carboxyl groups to aromatic carbon groups (D'Angelo, 2006).

C=O cont	(~1714)/(1800–1600)	Carbonyl contribution. Relative contribution of carbonyl/carboxyl groups (C=O) to combined contribution of oxygen-containing groups and aromatic carbon (C=C) structures.
C=C cont	(~1600)/(1800-1600)	Aromatic carbon contribution. Relative contribution of aromatic carbon groups (C=C) to combined contribution of oxygen-containing groups and aromatic carbon structures.
CHal/C=C	(3000–2800)/(1600–1500)	Aliphatic/aromatic carbon groups ratio. Relative contribution of aliphatic C–H stretching bands to aromatic carbon groups (C=C). Higher values indicate increasing aliphatic groups to aromatic carbon groups. This ratio is equivalent to the I1 index of Guo and Bustin (1998).
'A' Factor = CHal/(CHal+C=C)	(3000-2800)/ [(3000-2800)+(1600-1500)]	A Factor. Relative contribution of aliphatic C–H stretching bands to sum of aliphatic C–H stretching and aromatic carbon structures. According to Ganz and Kalkreuth (1987) it represents change in relative intensity of aliphatic groups.
'C' Factor = C=O/(C=O+C=C)	(1700-1600) / [(1700-1600)+(1600-1500)]	C Factor. Relative contribution of oxygen-containing compounds to sum of oxygen containing structures and aromatic carbon bands. According to Ganz and Kalkreuth (1987) it represents change in carbonyl/carboxyl groups.
CHal/C=O	(3000–2800)/(1800–1700)	Aliphatic/carbonyl groups ratio. Relative contribution of aliphatic C–H stretching bands to carbonyl/carboxyl groups (C=O). Indicator for cross-linking degree of a polymeric structure (i.e., the linking of polymer chains). Lower values indicate higher C=O content and higher cross-linking (Benítez et al., 2004).

Table 4. Morphological, anatomical, and ultrastructural characterization of the fossil taxa spectroscopically studied.

Fossil taxon	***Pseudoctenis ornata*** Archangelsky et al.	***Ginkgoites tigrensis*** Archangelsky	***Squamastrobus tigrensis*** Archangelsky and Del Fueyo	***Ptilophyllum micropapillosum*** Lafuente Diaz, Carrizo, and Del Fueyo	***Ruflorinia orlandoi*** Carrizo and Del Fueyo	***Ginkgoites skottsbergii*** Lundblad
	Archangelsky et al. 1995; Guignard, 2019	Archangelsky, 1965; Guignard, 2019	Archangelsky and Del Fueyo, 1989	Lafuente Diaz et al. 2019	Carrizo et al. 2014	Lundblad, 1971; Guignard et al. 2016; Guignard, 2019
Provenance	Punta del Barco Formation	Anfiteatro de Ticó Formation	Anfiteatro de Ticó Formation	Springhill Formation	Springhill Formation	Piedra Clavada/Kachaike Formation
Leaves						
General aspects	Pinnate	Simple, flabelliform	Scale-like, sessile and adpressed	Pinnate	At least bipinnate and imparipinnate	Simple, flabelliform
Pinnae / Leaflets / Segments		2-8 segmentos.	------			8-12 segments
Form and Arrangement	Linear to acuminate; opposite of sub-opposite	Lanceolate; obtuse and rounded apex		Falcate; opposite to sub-opposite; acute apex; lower margin decurrent	Alternate to sub-opposite	Lanceolate to linear; rounded apex
Pinnules	------	------	------	------		------
Number					6-7 pinnules	
Form and Arrangement					Oblong-lanceolate, obtuse to slightly acute apex	
Venation	Parallel	Open dichotomous	Uninerved	Parallel	Dichotomous	Open dichotomous
Adaxial Epidermis						
Ordinary epidermal cells	Smooth; epidermal cells of variable form	Smooth	Smooth	Smooth; markedly sinuous anticlinal walls	Weak cuticular striations; low hair density	Cells of variable form; straight anticlinal walls
Abaxial Epidermis						
General aspects	Numerous papillae in ordinary epidermal cells and subsidiary cells.	Smooth	Smooth	Numerous papillae, mainly simple and small. Sinuous anticlinal walls	Cuticular striations well-defined; high hair density	Smooth; straight anticlinal walls
Ordinary epidermal cells	Variable form	Rectangular and isodiametric	Rectangular and isodiametric	Rectangular in veins	Polygonal and variable size	Rectangular and isodiametric
Papillae	Numerous in ordinary epidermal cells. Also, in subsidiary cells.	------	Occasionally at the apex of the leaf	Numerous in ordinary epidermal cells. Also, in subsidiary cells.	Striated in subsidiary cells	In subsidiary cells
Hairs	------	------	------	------	Unicellular; simple or branched multicellulars	------
Stomatal Apparatuses	Hypostomatic	Amphistomatic	Amphistomatic	Hypostomatic	Hypostomatic	Amphistomatic
Form and size	Sub-circular to oval. Subsidiary cells arranged in concentric cycles and sunken guard cells	Cuadrangular; monocyclic to imperfectly dicyclic. 5-6 polyhedral subsidiary cells and sunken guard cells	Circular to oval; monocyclic to imperfectly dicyclic. 4-5 polygonal subsidiary cells and sunken guard cells. Florin ring	Quadrangular to subrectangular. Subsidiary cells occasionally with papillae and sunken guard cells	Circular to oval; monocyclic. 2-14 subsidiary cells with papillae and sunken guard cells	Oval to circular; monocyclic or partially dicyclic. 9-8 subsidiary cells with papillae and sunken guard cells
Arrangement	Irregular or in poorly defined rows	Random	In well-defined longitudinal rows	In 4-6 longitudinal rows	Grouped, 12-14 per group	Random
Cuticular Ultrastructure	A1–A2–B1 Layers	A1U–A1L–A2-B1 Layers	A2- B1 Layers	------	A2-B1-B2 Layers	A1U–A1L–A2-B1 Layers

Table 5. Terminology used to refer to chemical preservation types of plant fossils by means of FTIR spectroscopy studies.

Designation	Definition
Compression	It is defined considering an analogous model to that of the extant leaf anatomy: Compression = vitrinite (mesophyll) + cuticle (biomacropolymer). It is considered the most common preservation type of plant fossil remains (Zodrow et al., 2009).
Fossilized or macerated cuticle	It is less common than the compression preservation type. The origin of the fossilized cuticles is interpreted as the result of geochemical processes that involve maceration of compressions with sulfuric acid, after in situ pyritic oxidation. The coalified layer (vitrinitic component corresponding to the transformed mesophyll) is poorly preserved or only the cuticle itself is preserved. Fossilized cuticles are distinguished from other preservation types by: (a) varying shades of amber (fossils preserved as compression are broadly black), (b) general inability to fully separate into adaxial and abaxial epidermis, and (c) general lack of preservation of epidermal features such as anticline walls and stomatal apparatuses (Zodrow et al., 2009).
Cuticle-free coalified layer	Only the coalified layer, of mainly vitrinitic composition, is preserved without the cuticle; i.e., cuticle-free coalified layer correspond to the mesophyll transformed during a fossilization process that implied certain circumstances that prevented the preservation of the cuticular membranes [(e.g., Corystospermaceae from the Cacheuta Formation (Argentina) in Zodrow et al. (2009) and *Trigonocarpus ovules* in D'Angelo and Zodrow (2011)] Coalified layers occur in sediments that have a relatively higher level of thermal maturity than compressions

	(Zodrow et al., 2009).
Liptinitic compression	Considering the FTIR spectroscopic data belonging to ‘A’ and ‘C’ Factors (semiquantitative data) and the chemical similarity of the foliar compressions with respect to the liptinite maceral group (e.g., *Ptilophyllum micropapillosum* Lafuente Diaz et al., 2019)
Vitrinitic compression	Considering the FTIR spectroscopic data belonging to ‘A’ and ‘C’ Factors (semiquantitative data) and the chemical similarity of the foliar compressions with respect to the vitrinite maceral group (e.g., *Ginkgoites skottsbergii* Lafuente Diaz, 2019)

Figure 1

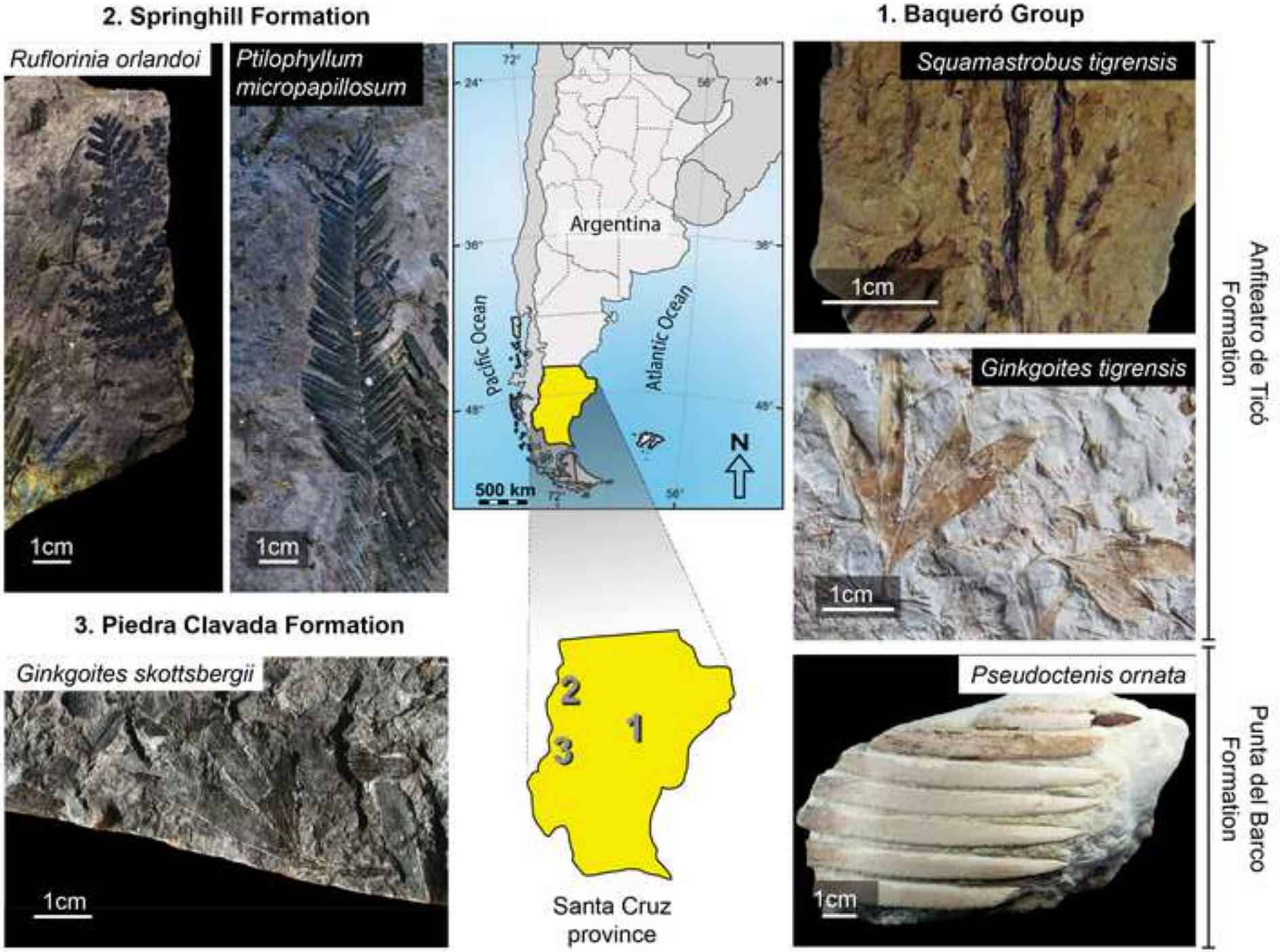

Figure 3

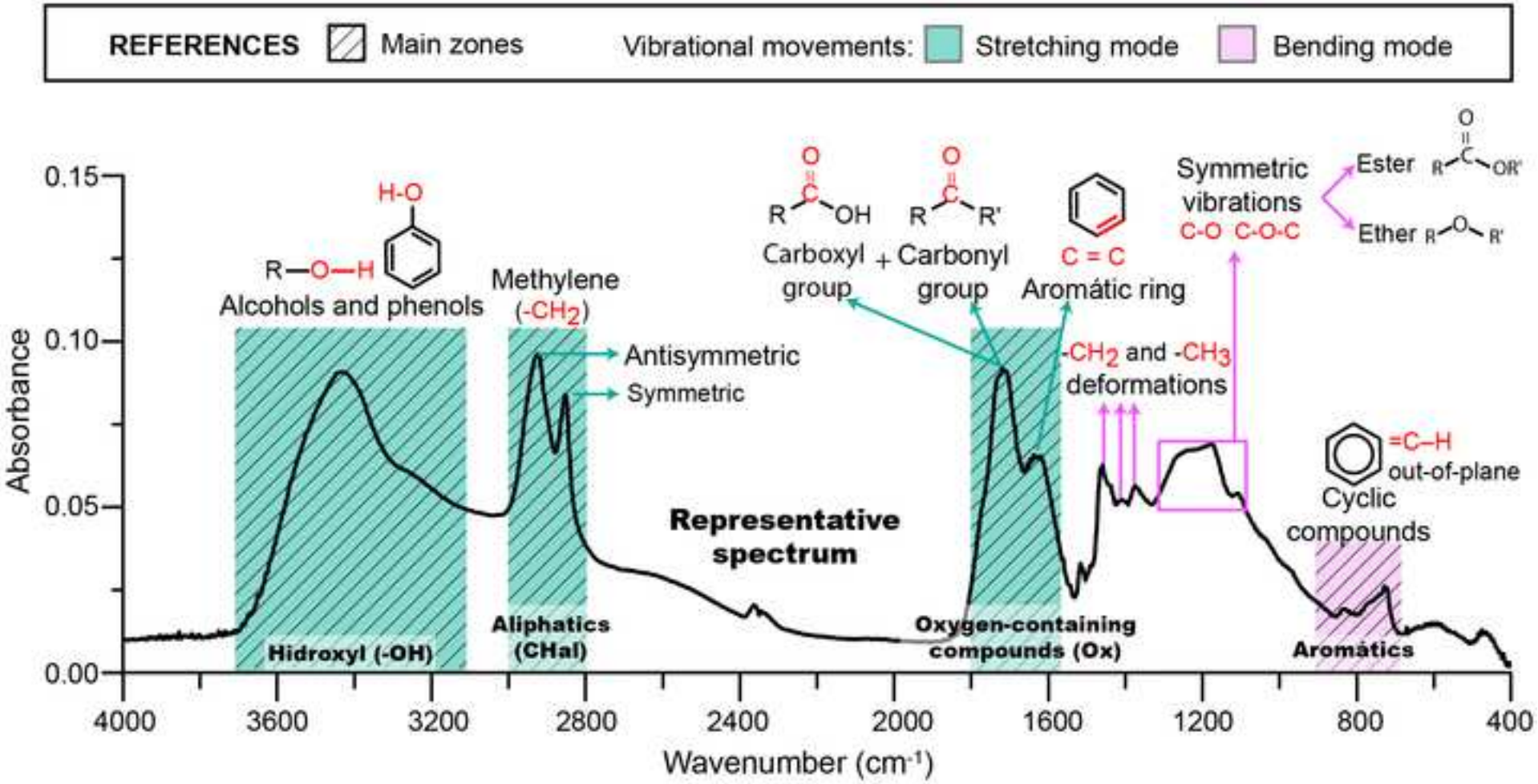

Figure 4

Click here to access/download;Figure;Lafuente Diaz et al. - Fig. 4.tif

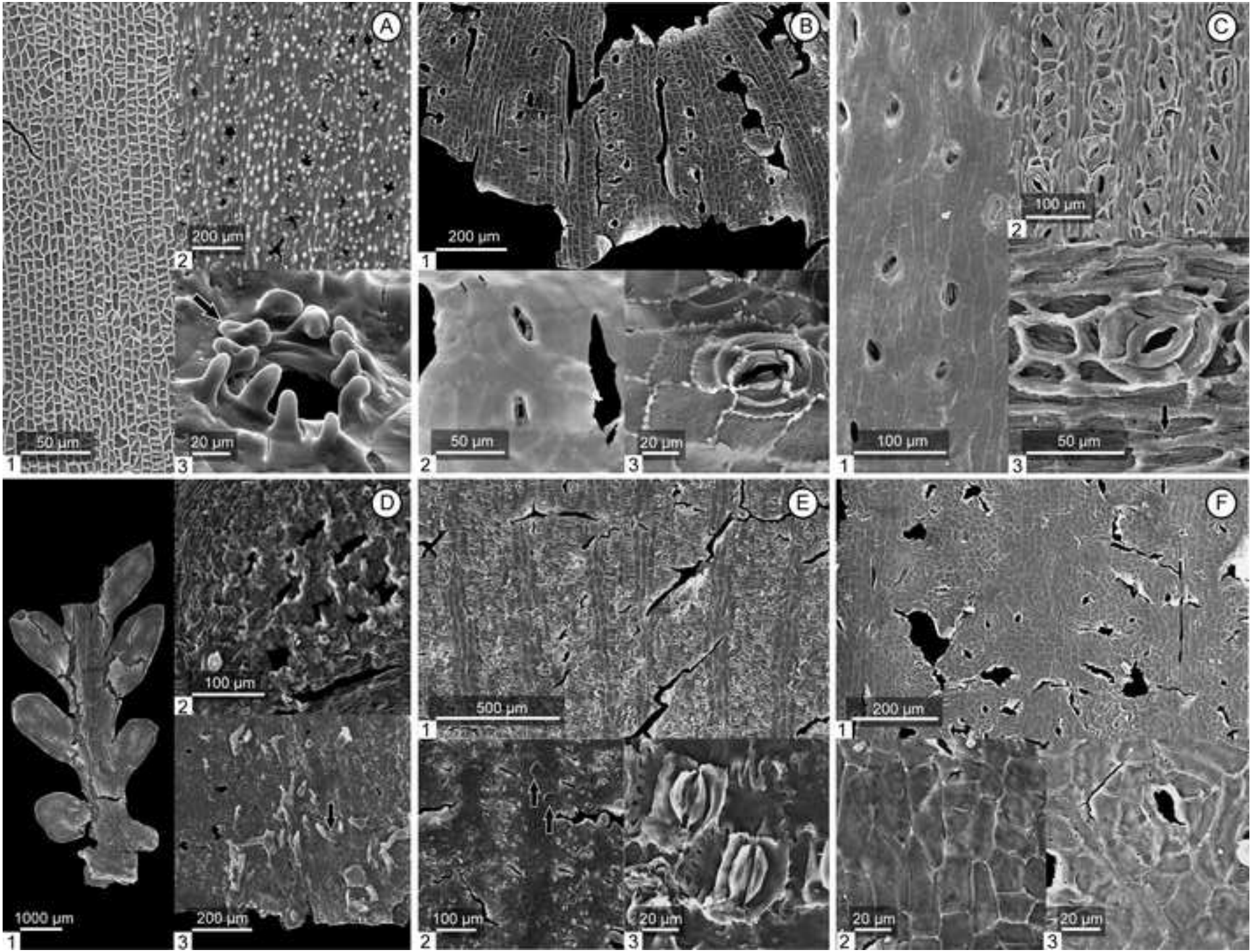

Figure 5

Click here to access/download;Figure;Lafuente Diaz et al. - Fig. 5 PCA.tif

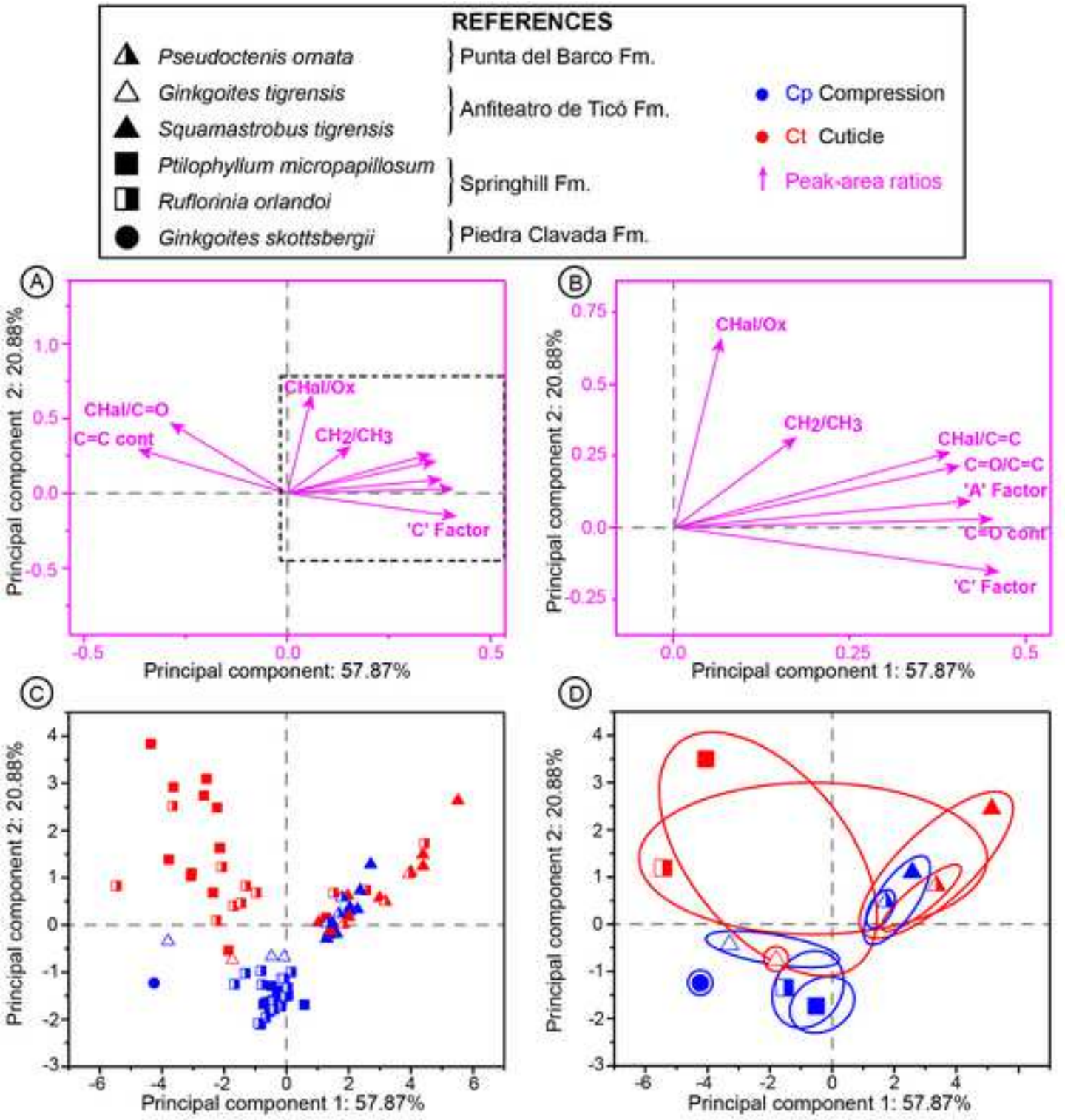

Figure 6

Click here to access/download;Figure;Lafuente Diaz et al. - Fig. 6.tif

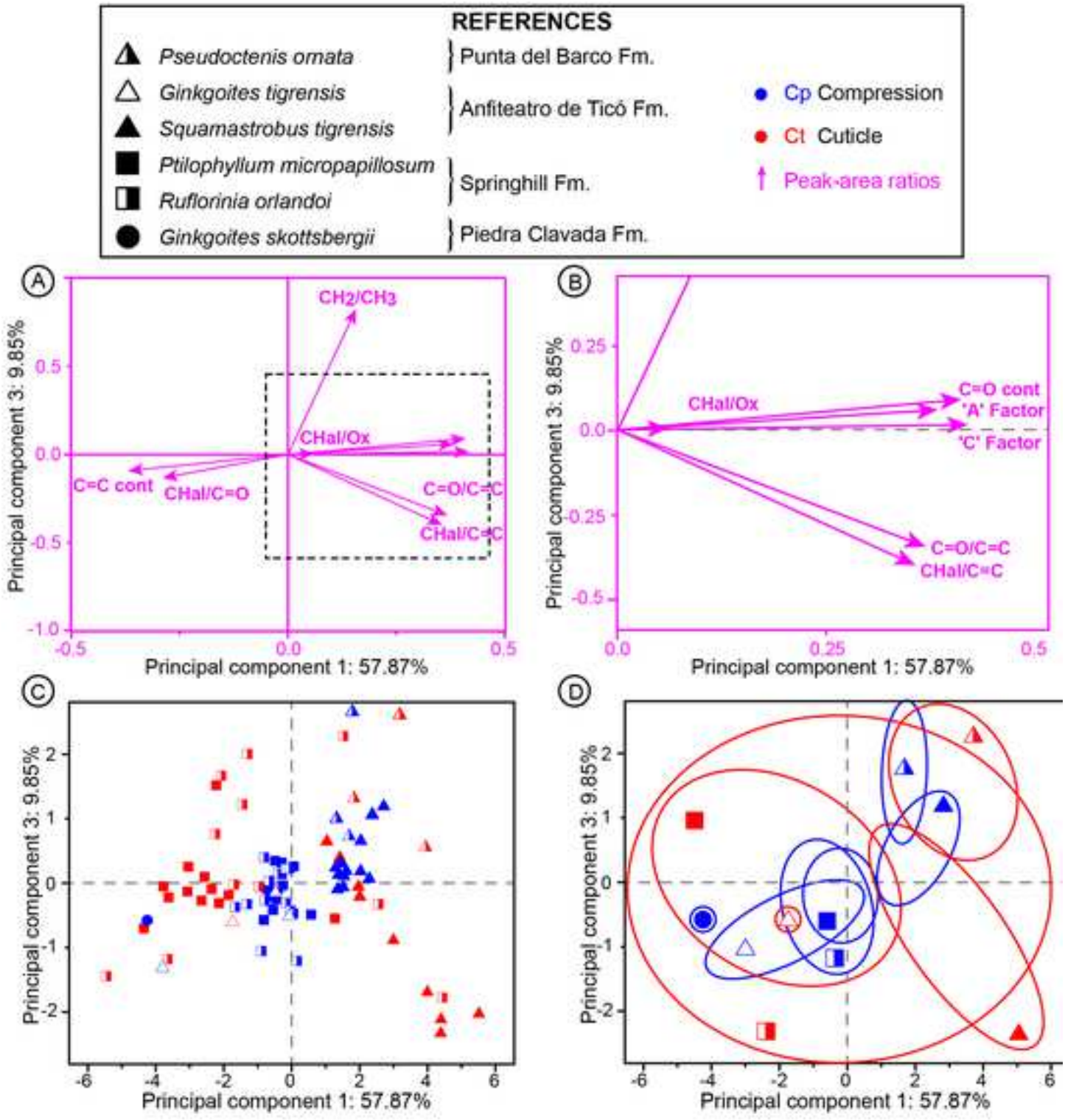

Figure 2

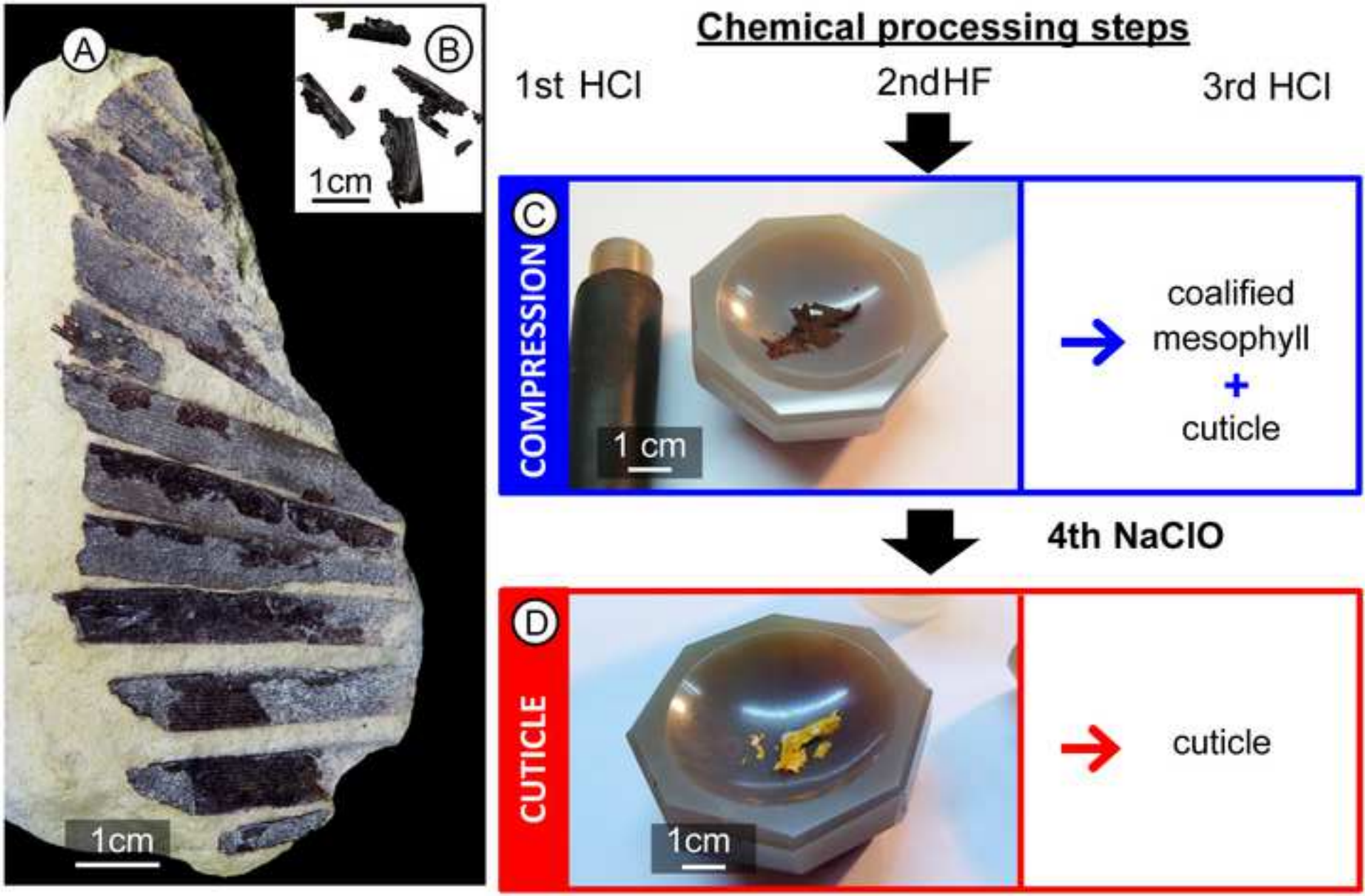

Figure 7

Click here to access/download;Figure;Lafuente Diaz et al. - Fig. 7.tif

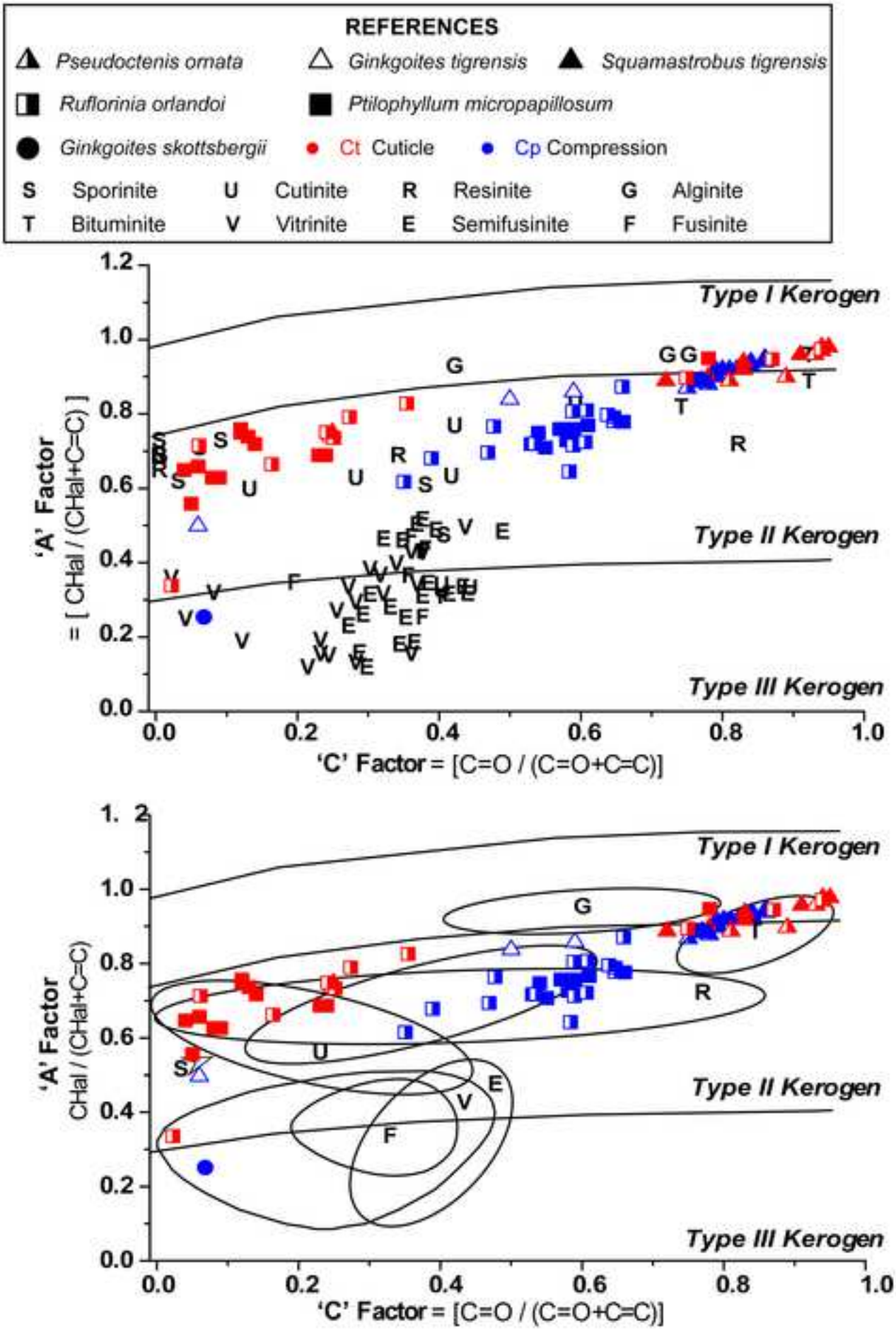

Appendix A – Supplementary data: FTIR spectra of the six Cretaceous gymnosperms fossil taxa from Argentina. Note Cp= compression (blue) and Ct= cuticle (red).

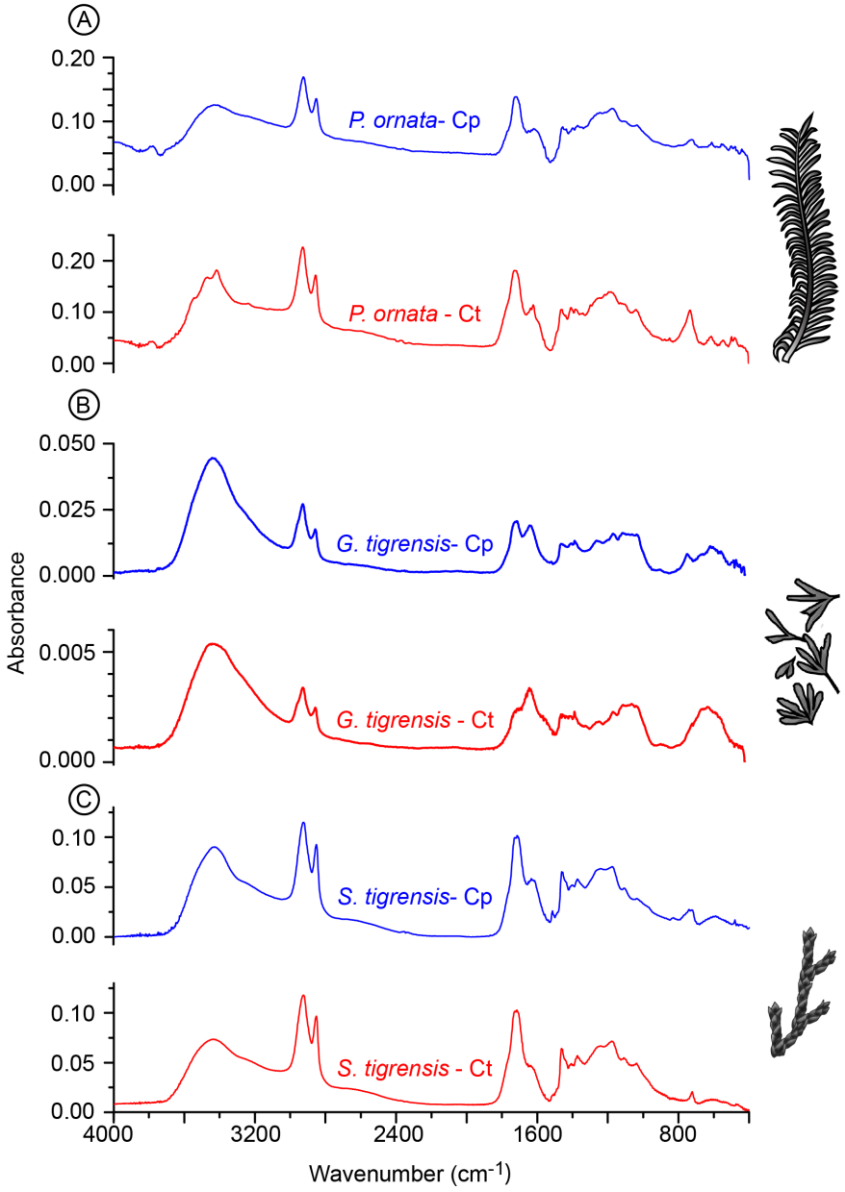

Figure A1. Representative FTIR spectra of the fossil taxa from the Baqueró Group. **A.** *Pseudoctenis ornata* Archangelsky et al., BA Pb 1220 (Cp2 and Ct2). **B.** *Ginkgoites tigrensis* Archangelsky, BA Pb 14883 (Cp1), 14887 (Ct4). **C.** *Squamastrobus tigrensis* Archangelsky and Del Fueyo, BA Pb11583 (Cp2 and Ct2). Data taken and modified from Lafuente Diaz (2019) and Lafuente Diaz et al. (2018a).

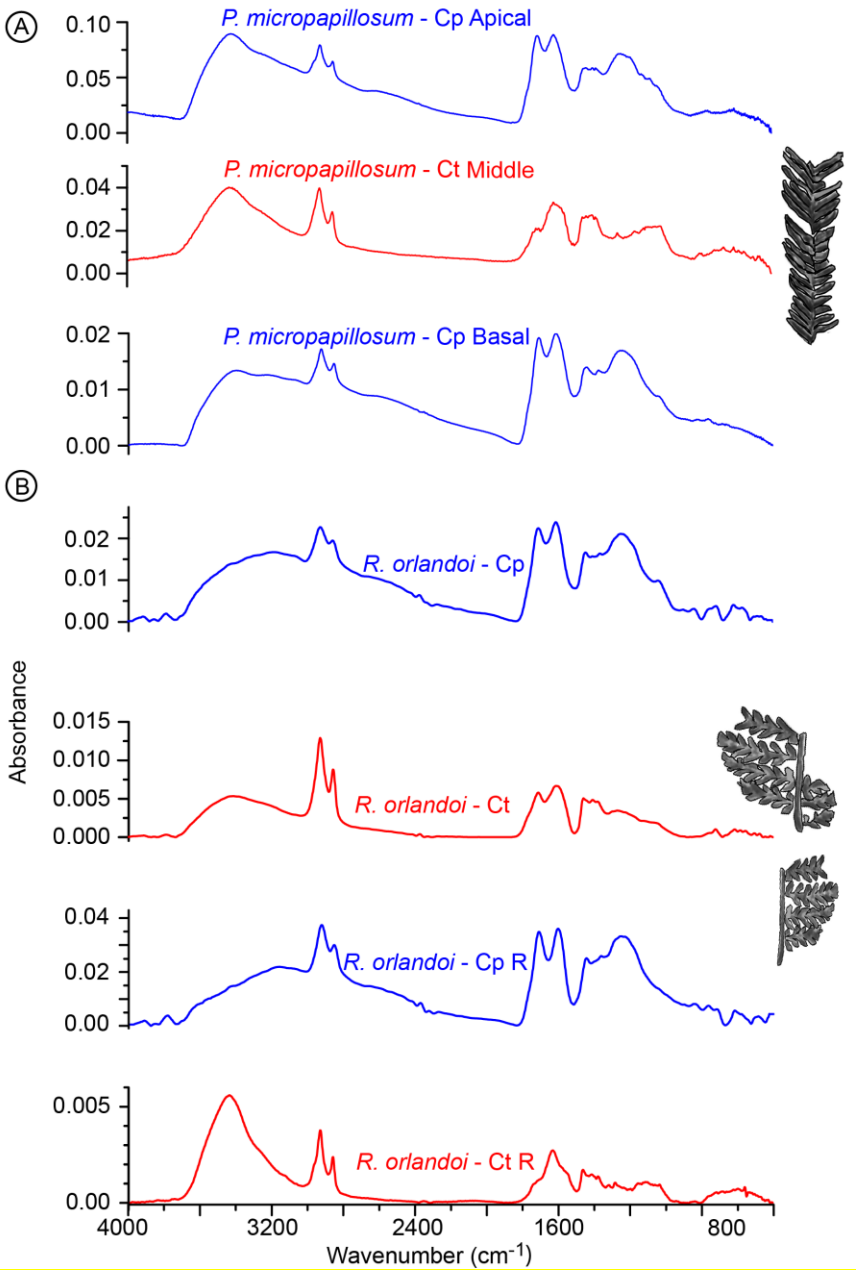

Figure A2. Representative FTIR spectra of the fossil taxa from the Springhill Formation. **A.** *Ptilophyllum micropapillosum* Lafuente Diaz et al., MPM Pb 15355. Note differential sampling among apical (2Cp-A), middle (2Ct-M) and basal (2Cp-B) frond parts. **B.** *Ruflorinia orlandoi* Carrizo and Del Fueyo, MPM Pb 15327. Note differential sampling between pinnae (Cp1 and Ct1) and rachis (Cp1 R and Ct1 R). Data taken and modified from Lafuente Diaz et al. (2019a, 2020).

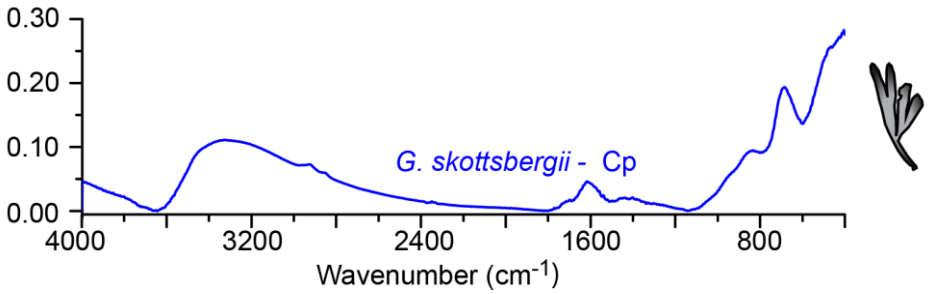

Figure A3. FTIR spectrum of the foliar compression from the Piedra Clavada/Kachaike Formation. *Ginkgoites skottsbergii*, BA Pb 13850. Data taken and modified from Lafuente Diaz (2019).

Appendix B

Fossil taxa	Samples	FTIR ratios / PCA variables								
		CH_2/CH_3	CHal/Ox	C=O/C=C	C=O cont	C=C cont	CHal/C=C	'A' Factor	'C' Factor	CHal/C=O
Squamastrobus tigrensis	Cp1	9.63	0.66	5.26	0.25	0.05	13.83	0.93	0.84	2.63
	Cp2	15.79	0.78	6.32	0.27	0.04	18.08	0.95	0.86	2.86
	Cp3a	7.69	0.61	4.12	0.22	0.05	11.40	0.92	0.80	2.77
	Cp3b	7.30	0.60	3.72	0.21	0.06	10.67	0.91	0.79	2.87
	Cp4a	8.58	0.57	4.24	0.22	0.05	11.25	0.92	0.81	2.65
	Cp4b	9.10	0.56	4.46	0.22	0.05	11.56	0.92	0.82	2.60
	Cp5	14.75	0.66	5.91	0.24	0.04	16.18	0.94	0.86	2.74
	Cp6	8.29	0.58	3.43	0.24	0.07	8.19	0.89	0.77	2.39
	Cp7a	8.27	0.60	3.67	0.22	0.06	10.14	0.91	0.79	2.76
	Cp7b	9.65	0.62	3.80	0.21	0.06	11.03	0.92	0.79	2.91
	Cp8	9.87	0.65	6.29	0.25	0.04	16.06	0.94	0.86	2.55
	Cp9	12.27	0.62	5.24	0.22	0.04	14.63	0.94	0.84	2.79
	Ct2	11.56	0.84	20.39	0.33	0.02	51.41	0.98	0.95	2.52
	Ct3	6.69	0.70	16.88	0.33	0.02	35.99	0.97	0.94	2.13
	Ct4a	7.61	0.68	9.53	0.28	0.03	23.08	0.96	0.91	2.42
	Ct4b	7.56	0.69	14.56	0.30	0.02	33.66	0.97	0.94	2.31
	Ct6	6.90	0.71	4.99	0.31	0.06	11.54	0.92	0.83	2.31
	Ct7a	9.23	0.59	3.62	0.24	0.07	8.93	0.90	0.78	2.47
	Ct7b	7.07	0.72	16.42	0.28	0.02	42.82	0.98	0.94	2.61
	Ct8	8.58	0.78	4.77	0.25	0.05	15.11	0.94	0.83	3.17
	Ct9	10.22	0.63	2.63	0.21	0.08	8.08	0.89	0.72	3.07
Pseudoctenis ornata	Cp1	10.95	0.66	3.85	0.27	0.07	9.39	0.90	0.79	2.44
	Cp2	11.59	0.60	2.99	0.27	0.09	6.78	0.87	0.75	2.27
	Cp3	20.12	0.57	3.46	0.26	0.08	7.51	0.88	0.78	2.17
	Ct1	16.47	0.56	13.72	0.31	0.02	24.35	0.96	0.93	1.78
	Ct2	13.62	0.54	4.25	0.29	0.07	7.89	0.89	0.81	1.86
	Ct3	20.90	0.47	7.78	0.42	0.05	8.76	0.90	0.89	1.13
Ginkgoites tigrensis	Cp1	4.17	0.54	1.44	0.13	0.09	6.07	0.86	0.59	4.21
	Cp2	1.88	0.35	0.06	0.02	0.35	1.01	0.50	0.06	16.82
	Cp3	5.97	0.48	0.99	0.09	0.09	5.15	0.84	0.50	5.21
	Ct4	4.03	0.42	0.33	0.04	0.14	3.07	0.75	0.25	9.24

Continues next page

Fossil taxa	Samples	FTIR ratios / PCA variables								
		CH_2/CH_3	CHal/Ox	C=O/C=C	C=O cont	C=C cont	CHal/C=C	'A Factor'	'C' Factor	CHal/C=O
Ruflorinia orlandoi	Cp1	4.92	0.36	0.91	0.10	0.11	3.30	0.77	0.48	3.61
	Cp1 R	8.07	0.38	0.88	0.15	0.16	2.30	0.70	0.47	2.61
	Cp2	7.42	0.36	1.43	0.12	0.09	4.21	0.81	0.59	2.94
	Cp2 R	0.86	0.25	1.15	0.11	0.10	2.58	0.72	0.54	2.25
	Cp3	0.76	0.54	1.93	0.15	0.08	6.89	0.87	0.66	3.57
	Cp4	7.42	0.37	1.55	0.13	0.09	4.28	0.81	0.61	2.76
	Cp4 R	4.64	0.41	0.64	0.12	0.19	2.14	0.68	0.39	3.37
	Cp5	4.51	0.35	0.54	0.12	0.21	1.62	0.62	0.35	3.00
	Cp5 R	3.96	0.35	1.83	0.18	0.10	3.57	0.78	0.65	1.95
	Cp6	3.72	0.40	1.83	0.19	0.11	3.80	0.79	0.65	2.07
	Cp7a	4.78	0.27	1.76	0.12	0.07	3.96	0.80	0.64	2.25
	Ct7b	6.74	0.26	1.43	0.15	0.10	2.52	0.72	0.59	1.76
	Ct8	5.64	0.24	1.54	0.14	0.09	2.63	0.72	0.61	1.71
	Cp8 R	6.16	0.19	1.40	0.15	0.11	1.82	0.65	0.58	1.30
	Ct1	10.37	0.74	0.38	0.07	0.19	3.81	0.79	0.27	10.13
	Ct1 R	3.96	0.80	0.06	0.02	0.32	2.52	0.72	0.06	38.83
	Ct2	12.98	0.55	0.32	0.06	0.19	2.91	0.74	0.24	8.97
	Ct3	16.84	0.58	0.34	0.07	0.21	2.79	0.74	0.25	8.31
	Ct5	15.65	0.64	0.20	0.06	0.32	1.99	0.67	0.16	10.16
	Ct5 R	3.10	0.38	0.02	0.02	0.73	0.51	0.34	0.02	22.31
	Ct6	18.46	0.63	2.98	0.21	0.07	8.76	0.90	0.75	2.94
	Ct7a	8.15	0.82	15.47	0.33	0.02	38.08	0.97	0.94	2.46
	Ct7b	8.19	0.79	6.70	0.29	0.04	18.05	0.95	0.87	2.70
	Ct8	6.66	0.79	0.55	0.09	0.16	4.83	0.83	0.35	8.80
	Ct8 R	6.90	0.66	0.32	0.07	0.22	3.03	0.75	0.24	9.54

Continues next page

Fossil taxa	Samples	FTIR ratios / PCA variables								
		CH_2/CH_3	CHal/Ox	C=O/C=C	C=O cont	C=C cont	CHal/C=C	'A' Factor	'C' Factor	CHal/C=O
Ptilophyllum micropapillosum	2-Cp A	3.27	0.21	1.22	0.10	0.09	2.40	0.71	0.55	1.96
	2-Cp M	5.02	0.25	3.39	0.11	0.03	7.79	0.89	0.77	2.30
	2-Cp B	5.69	0.26	1.11	0.11	0.10	2.53	0.72	0.53	2.27
	6-Cp A	4.89	0.30	1.34	0.13	0.09	3.21	0.76	0.57	2.39
	6-Cp M	5.61	0.28	1.40	0.13	0.10	2.91	0.74	0.58	2.08
	6-Cp B	5.98	0.30	1.53	0.14	0.09	3.41	0.77	0.61	2.22
	8-Cp A	7.44	0.28	1.96	0.16	0.08	3.45	0.78	0.66	1.76
	8-Cp M	5.15	0.28	1.16	0.11	0.09	2.97	0.75	0.54	2.57
	8-Cp B	4.02	0.26	1.38	0.13	0.09	2.76	0.73	0.58	2.00
	11-Cp A	6.81	0.30	1.47	0.14	0.09	3.16	0.76	0.59	2.16
	11-Cp M	7.67	0.30	1.42	0.14	0.10	3.03	0.75	0.59	2.14
	11-Cp B	7.85	0.32	1.18	0.12	0.11	2.97	0.75	0.54	2.53
	2-Ct A	7.09	0.63	3.52	0.12	0.03	19.15	0.95	0.78	5.44
	2-Ct M	7.54	0.62	0.10	0.04	0.36	1.74	0.63	0.09	17.51
	2-Ct B	9.53	0.57	0.09	0.03	0.34	1.71	0.63	0.08	19.02
	6-Ct A	8.82	1.16	0.15	0.06	0.40	2.89	0.74	0.13	19.47
	6-Ct M	5.68	0.98	0.29	0.13	0.45	2.20	0.69	0.23	7.49
	6-Ct B	7.20	0.97	0.04	0.02	0.53	1.84	0.65	0.04	41.72
	8-Ct A	7.15	1.06	0.14	0.05	0.34	3.09	0.76	0.12	22.90
	8-Ct M	15.87	0.81	0.14	0.04	0.26	3.08	0.75	0.12	22.76
	8-Ct B	5.84	0.45	0.32	0.06	0.20	2.28	0.69	0.24	7.08
	11-Ct A	8.77	0.56	0.06	0.02	0.45	1.25	0.56	0.05	22.76
	11-Ct M	7.19	0.61	0.16	0.04	0.23	2.59	0.72	0.14	15.91
	11-Ct B	8.38	0.90	0.07	0.03	0.46	1.98	0.66	0.06	29.83
Ginkgoites skottsbergii	Cp1	5.28	0.17	0.07	0.04	0.49	0.34	0.26	0.07	4.71

End of table

Table B1. Semi-quantitative FTIR data set of the six analyzed gymnosperms from the province of Santa Cruz, Argentina. Note that Cp and Ct correspond to compression and cuticle, respectively. In turn, the letters "a" and "b" indicate duplicate samples. In the case of *R. orlandoi* samples the letter R indicates rachis whereas those of *P. micropapillosum* the letters A, M, and B correspond to apical, middle, and basal frond parts, respectively.

Appendix C – Supplementary data: Solution of principal component analysis (PCA)

Table C1. Input correlation matrix of nine variables with unity in the principal diagonal. Data set includes the following sample forms: (1) compression, (2) cuticle belonging to *Ginkgoites tigrensis, Pseudoctenis ornata*, *Squamastrobus tigrensis*, *Ruflorinia orlandoi*, *Ptilophyllum micropapillosum*, and *Ginkgoites skottsbergii*.

	CH_2/CH_3	CHal/Ox	C=O/C=C	C=O cont	C=C cont	CHal/C=C	'A' Factor	'C' Factor	CHal/C=O
CH_2/CH_3	1	0.35685	0.26032	0.40734	-0.15819	0.22152	0.32008	0.23598	-0.06740
CHal/Ox	0.35685	1	0.28430	0.16138	0.19897	0.37625	0.30460	-0.04607	0.44710
C=O/C=C	0.26032	0.28430	1	0.78224	-0.50770	0.97218	0.63568	0.70273	-0.34275
C=O cont	0.40734	0.16138	0.78224	1	-0.70817	0.71062	0.76627	0.90958	-0.60888
C=C cont	-0.15819	0.19897	-0.50770	-0.70817	1	-0.48292	-0.78307	-0.87990	0.78308
CHal/C=C	0.22152	0.37625	0.97218	0.71062	-0.48292	1	0.65777	0.66471	-0.28401
'A' Factor	0.32008	0.30460	0.63568	0.76627	-0.78307	0.65777	1	0.82716	-0.41698
'C' Factor	0.23598	-0.04607	0.70273	0.90958	-0.87990	0.66471	0.82716	1	-0.74365
CHal/C=O	-0.06740	0.44710	-0.34275	-0.60888	0.78308	-0.28401	-0.41698	-0.74365	1

Table C2. Solution of PCA including FTIR data from *Ginkgoites tigrensis. Pseudoctenis ornata*. *Squamastrobus tigrensis*. *Ruflorinia orlandoi*. *Ptilophyllum micropapillosum*, and *Ginkgoites skottsbergii*

	PC 1	PC 2	PC 3	PC 4	PC 5	PC 6	PC 7	PC 8	PC 9
CH_2/CH_3	0.359115	0.433720	0.777624	-0.251121	0.115537	0.039382	0.010495	0.012376	-0.000043
CHal/Ox	0.138112	0.909803	0.005155	0.269979	-0.246777	0.131614	-0.040786	0.016052	0.011211
C=O/C=C	0.839770	0.295300	-0.325021	-0.298155	0.079623	0.005538	-0.022461	-0.051947	0.058957
C=O cont	0.935940	0.040496	0.084310	-0.088888	-0.201963	-0.242204	-0.054752	-0.062644	-0.031518
C=C cont	-0.843790	0.402964	-0.087636	-0.232614	-0.145175	-0.132383	0.158541	0.008704	0.006164
CHal/C=C	0.811768	0.361670	-0.376984	-0.199377	0.093093	0.115820	0.035979	0.042791	-0.056152
‘A’ Factor	0.871622	0.126644	0.056124	0.424528	0.139280	-0.041021	0.128100	-0.058017	0.002263
‘C’ Factor	0.954101	-0.212218	0.014354	0.068403	-0.047378	-0.128307	0.016377	0.142051	0.024824
CHal/C=O	-0.661691	0.648006	-0.126233	0.125817	0.241066	-0.214855	-0.074445	0.025331	-0.005414
Eigenvalue	5.208053	1.878868	0.886560	0.527342	0.230875	0.172814	0.053925	0.033126	0.008437
Cumulative explained variance %	57.8673	78.7436	88.5942	94.4536	97.0189	98.9390	99.5382	99.9063	100

Table C3. Acceptable three-component solution of PCA for *Pseudoctenis ornata*. *Ginkgoites tigrensis. Squamastrobus tigrensis*. *Ptilophyllum micropapillosum. Ruflorinia orlandoi*, and *Ginkgoites skottsbergii*

	PC 1	**PC 2**	**PC 3**	**Variance***
CH_2/CH_3	0.359115	0.433720	0.777624	92.18
CHal/Ox	0.138112	0.909803	0.005155	84.68
C=O/C=C	0.839770	0.295300	-0.325021	89.81
C=O cont	0.935940	0.040496	0.084310	88.47
C=C cont	-0.843790	0.402964	-0.087636	88.20
CHal/C=C	0.811768	0.361670	-0.376984	93.19
Factor 'A'	0.871622	0.126644	0.056124	77.89
Factor 'C'	0.954101	-0.212218	0.014354	95.56
CHal/C=O	-0.661691	0.648006	-0.126233	87.37
Eigenvalue r	5.208053	1.878868	0.886560	7.973481
Cumulative explained variance %	57.8673	78.7436	88.5942	

* Variance explained by first 3 PC (%).